NASA CR-66403

XLA-11227

GENERAL AMERICAN TRANSPORTATION CORPORATION

GATX

ADVANCED CONCEPT OF A LABORATORY-TYPE OXYGEN RECLAMATION SYSTEM FOR MANNED SPACECRAFT

By A. J. Glueckert
G. A. Remus

Prepared under Contract No. NAS 1-5269 by
GENERAL AMERICAN RESEARCH DIVISION
GENERAL AMERICAN TRANSPORTATION CORPORATION
Niles, Illinois 60648

for Langley Research Center

NATIONAL AERONAUTICS AND SPACE ADMINISTRATION

ABSTRACT

Three processes comprising an oxygen reclamation system were investigated: (1) electrolytic reduction of carbon dioxide in a molten carbonate electrolysis cell, (2) oxygen permeation through a heated silver membrane, and (3) catalytic disproportionation of carbon monoxide to carbon and carbon dioxide.

The electrolysis cell effectively reduced carbon dioxide giving essentially theoretical yields of oxygen at the operating temperature of 1300°F. The electrolyte was a molten mixture of the carbonates of sodium, lithium and potassium immobilized by magnesium oxide to form a non-flowing matrix. Quantitative reduction of CO_2 could not be related to the power input due to cell body corrosion and electrolyte cross-leakage problems. These same problems prevented fabrication of a fully operational cell; due to a shift in emphasis to fabrication of the catalytic reactor, all of the research planned for this component was not completed.

A silver foil membrane corroded and leaked, when used as a direct contact anode in the electrolysis cell, obviating its use as an oxygen separation device in that location. Further tests of the silver foil, not as an electrode, but as a separation membrane showed that pure silver, at 1300° to 1400°F, leaks gas through fissures which develop along grain boundaries. However, a magnesium-nickel alloy of silver continuously separated pure oxygen from a mixture with carbon dioxide for 60 days without cross-leakage.

The catalytic reactor effectively disproportionated carbon monoxide to carbon dioxide and carbon. The most effective catalyst was H-219 nickel oxide prepared by the Girdler Catalyst Division of the Chemetron Corporation. Conversion averaged 85% of theoretical with pure CO feed, and 52% with a 1:1 mixture of CO and CO_2. A one-tenth man capacity laboratory model was fabricated and operated continuously for eight days with the 1:1 CO and CO_2 feed mixture.

FOREWORD

This report summarizes the work accomplished under Contract NAS1-5269 for research and development of a system which reclaims oxygen from carbon dioxide for use on manned spacecraft. This work was initiated on 23 June, 1965 and completed on 15 March 1967. The program was performed by the General American Research Division of the General American Transportation Corporation, 7449 Natchez Avenue, Niles, Illinois 60648. The work was monitored by Mr. Rex B. Martin, National Aeronautics and Space Administration, Langley Research Center, Langley Station, Hampton, Virginia 23365.

The work reported herein was performed by personnel within the Atmosphere Control Section of GARD's Life-Support Systems Group, under the direction of Mr. R. A. Bambenek and supervision of Mr. G. A. Remus; Mr. A. J. Glueckert served as project engineer.

TABLE OF CONTENTS

LIST OF FIGURES

LIST OF FIGURES (continued)

LIST OF FIGURES (continued)

LIST OF TABLES

SECTION 1

INTRODUCTION AND SUMMARY

The three concepts investigated during this contract were: (1) the reduction of carbon dioxide in a molten carbonate electrolysis cell, (2) the selective permeation of oxygen through a silver membrane and, (3) the catalytic disproportionation of carbon monoxide to carbon dioxide and carbon. These three processes can be integrated into a system which converts carbon dioxide into carbon and oxygen. The flow sheet in Figure 1 shows quantities and compositions of the gases in a one man capacity integrated system. The minus (-) sign in a block signifies that the component is consumed in the cell while a plus (+) sign means the component is produced in the cell. The quantities of A and B recycle gases are dependent upon the average conversion of carbon dioxide in the electrolysis cell and the average conversion of carbon monoxide in the catalytic reactor. If all of the carbon dioxide which is in the anode stream of the electrolysis cell is returned to the recycle loop the CO_2 feed gas rate will be 0.1 lb/hr. However, if the oxygen-carbon dioxide separator is not used and the carbon dioxide is dumped into the cabin, the CO_2 feed gas rate must be increased to 0.3 lb/hr.

1.1 Laboratory Studies

Laboratory bench scale tests were conducted on all three processes. The electrochemical reduction cell developed a number of problems due primarily to corrosion of the cell housing materials by the electrolyte at 1300°F. A silver membrane for selective oxygen permeation was operated continuously for two months without failure or shutdown. Sufficient design data was obtained to scale

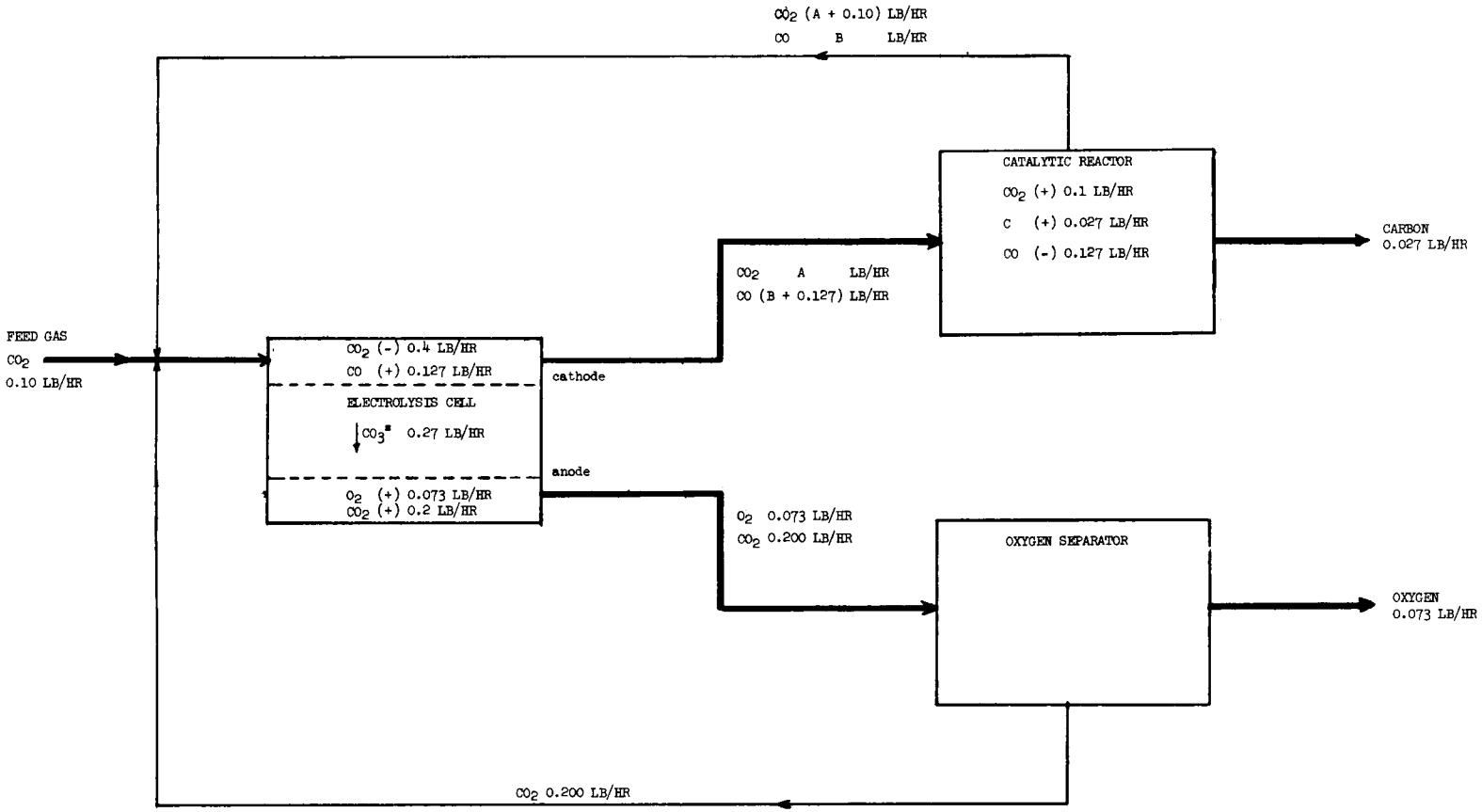

Figure 1 FLOW SHEET OF INTEGRATED OXYGEN RECLAMATION SYSTEM (1 MAN CAPACITY)

up to a larger unit, but better alloys are required to improve operating life beyond two months.

A large number of catalyst were evaluated under a variety of parameters in the study of catalytic disproportionation of carbon monoxide to carbon and carbon dioxide. The most efficient catalyst (based on activity and weight ratio of carbon/catalyst) was found to be a granular nickel oxide intermediate made by the Girdler Catalyst Division of the Chemetron Corporation and identified as H-219. This catalyst was tested with different gas mixtures and sufficient data was obtained to design and build a 0.1 man capacity laboratory model.

1.2 Laboratory-Type Catalytic Reactor

A prototype reactor was designed, constructed, and tested for the disproportionation of carbon monoxide to carbon dioxide and carbon because this concept was the most advanced of the three studied. The specifications for this reactor were:

1. The capacity should be equivalent to 0.1 man capacity, i.e., provide for conversion of .010 lb CO_2 per hr to .0073 lb O_2 and .0027 lb of carbon per hr. The reactor thus converts .0127 lb of carbon monoxide to balance the generation of .0027 lb of carbon and .010 lb CO_2 per hr.
2. The average shutdown time to change reactor canisters should not exceed 1 hour per 24 hour period.
3. The amount of carbon carried from the reactor cell by the gas stream is normally to be less than 0.1 percent of the carbon which is formed.

1.3 Reactor Performance

The catalytic reactor performance exceeded all three of the above specifications.

The average conversion was 52.1 percent of the input carbon monoxide; thus, 0.0034 lbs of carbon and 0.0125 lbs of carbon dioxide were produced per hour equivalent to 1/8 man capacity.

The reactor was operated continuously for eight days; then it was shut down to switch reactor canisters. Four hours were spent between the shut-off time and the time a new reactor was installed and brought to operating temperature. Therefore, the average rate of shutdown time is 0.5 hours per 24 hour period.

No carbon was found to have been swept out of the reactor during operation. A plug of quartz wool and 5.0 micron pore size ceramic filter effectively prevent carbon entrainment.

SECTION 2

ELECTROCHEMICAL REDUCTION OF CARBON DIOXIDE

2.1 Background

Electrolytic reduction of carbon dioxide to carbon monoxide and oxygen can be made to take place in a cell in which the electrolyte is a molten mixture of carbonates. The reaction must be carried out at a temperature which is high enough to minimize the formation of elemental carbon on the cathode. As seen in Figure 2, low temperatures enhance the formation of carbon while at temperatures near 1300°F and above the change in equilibrium favors the formation of carbon monoxide which is subsequently converted to carbon dioxide and carbon over a suitable catalyst.

2.1.1 Reactions and Products

The reactions which take place in the electrolysis cell are:

(1) Cathode (-) $4CO_2 + 4e^- \longrightarrow 2CO + 2CO_3^=$

(2) Anode (+) $2CO_3^= \longrightarrow O_2 + 2CO_2 + 4e^-$

Overall $2CO_2 \longrightarrow 2CO + O_2$

As explained in the previous paragraph, low temperatures (< 1300°F) allow carbon to form on the cathode according to the equation:

(3) $3CO_2 + 4\bar{e} \longrightarrow C + 2CO_3^=$ and the overall equation becomes

(4) $CO_2 \longrightarrow C + O_2$.

The purpose of operating at higher temperatures and forming carbon monoxide at the cathode is (1) to eliminate the need to periodically shut down the

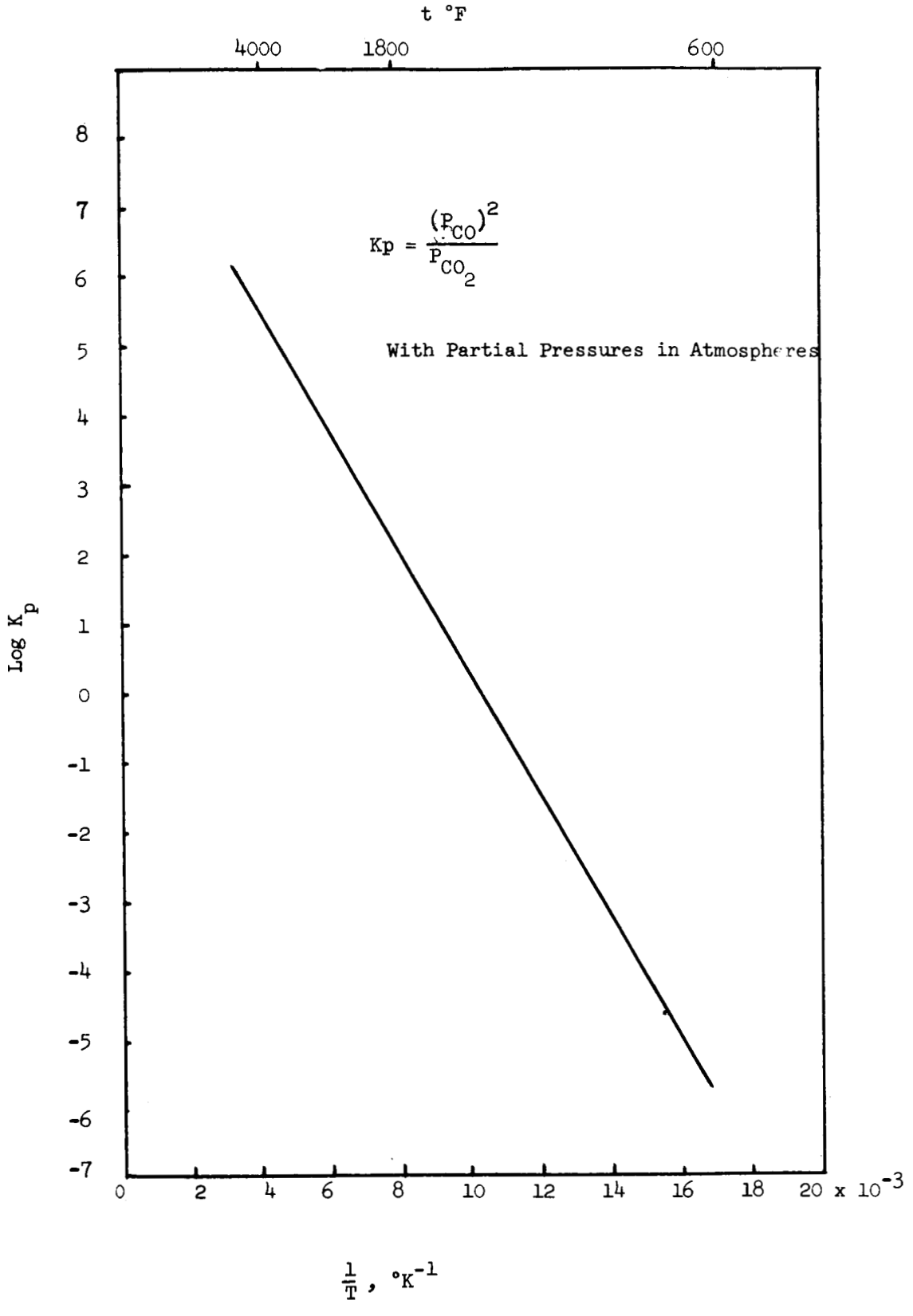

Figure 2 EQUILIBRIUM FOR THE REACTION $C + CO_2 \longrightarrow 2CO$ AS A FUNCTION OF TEMPERATURE

reactor in order to remove carbon from the electrode and (2) prevent carbon from being mixed with the electrolyte and shorting the cell. The products formed at the cathode, according to equation 1, cannot be released into a manned environment because of the presence of carbon monoxide. This can be catalytically converted to carbon dioxide and carbon and is discussed in Section 4 of this report. The oxygen and carbon dioxide mixture which is formed at the anode, equation 2, can be directly returned to the cabin atmosphere at the expense of an increase in the size of the CO_2 remover, or the oxygen and carbon dioxide can be separated. One such separation technique, namely selective permeation of oxygen through silver, is discussed in Section 3 of this report.

2.1.2 Electrolyte

The electrolyte used in this program consisted of a mixture of equal quantities by weight of lithium carbonate, sodium carbonate and potassium carbonate plus a variable quantity of magnesium oxide. The purpose of using a mixture of carbonates is to decrease the melting point of the electrolyte; the purpose of the magnesium oxide powder is to immobilize the molten carbonates for application in a weightless environment. Table 1 lists the melting points of various carbonates and carbonate mixtures. The reason for operating with molten carbonates is that electrical resistance decreases with increasing temperatures and the molten state is necessary to transport carbonate ions. Table 2 shows typical resistance values for a 1:1:1 (weight) mixture of lithium, potassium and sodium carbonates which were absorbed in a 1" o.d. x 12" x 1/8" wall porous aluminum oxide tube that had electrodes attached to the inner and outer surfaces.

Table 1

MELTING POINT OF CARBONATE ELECTROLYTES

COMPOUND		MELTING POINT °F	SOURCE
Li_2CO_3		1142	Handbook*
K_2CO_3		1634	"
Na_2CO_3		1562	"
Li_2CO_3 K_2CO_3 Na_2CO_3	equal portions by weight	750	experimental
Li_2CO_3 K_2CO_3	equal portions by weight	900	experimental
K_2CO_3 Na_2CO_3	equal portions by weight	1300	experimental
1 part (wt) Li_2CO_3 1 part (wt) K_2CO_3 1 part (wt) Na_2CO_3 3 parts (wt) MgO		750	experimental

*Handbook of Chemistry and Physics, 42nd Edition, The Chemical Rubber Publishing Company, 1960.

Table 2

RESISTANCE OF CARBONATE ELECTROLYTE

Temperature °F	Resistance - Ohms
280	not measureable
390	2×10^6
440	9×10^5
550	24
700	11
790	4.5
800	2.1
890	1.5

A significant decrease in resistance was observed before the electrolyte reached its melting point of 750°F.

The viscosity of the molten carbonate mixture is controlled by the amount of magnesium oxide in the electrolyte formulation. Original experiments contained 50 percent (by weight) magnesium oxide; however, this electrolyte was too viscous and would not seal adequately to prevent cross leakage between the cathode and anode gas streams. A mixture which contains between 30 to 35 percent magnesium oxide has a sufficiently high viscosity at 1300°F so that it will not flow through an 80 mesh platinum screen electrode, and is sufficiently fluid to prevent mixing of the cathode and anode gas streams.

2.1.3 Materials of Construction

2.1.3.1 Cell Housing - None of the materials used were completely inert to the attack of the molten carbonates at 1300°F; however, certain materials minimize the attack, and are suitable for tests which last for no more than several weeks. The properties which are required for materials which are in contact with the carbonate are listed below.

1. Inert to chemical attack by the molten carbonate
2. Negligible electrical conductivity at the operating temperature
3. Ability to be wetted by the molten carbonate to stop gas leakage.

Table 3 summarizes the results of tests with various materials.

Table 3

RESISTANCE OF MATERIALS TO MOLTEN CARBONATES AT 1300°F

	Materials	Degree of Attack
1.	Pyrex and Vycor	Severe attack
2.	Stainless housing coating with various enamels, frits, procelains, and high temperature ceramic coatings	Severe to moderate attack
3.	Flame sprayed aluminum oxide on stainless steel (Rokide A)	Severe attack
4.	Nucerite (Pfaudler Co.)	Moderate attack - discoloration of electrolyte
5.	Solid boron nitride	Mild attack
6.	Impervious zirconium oxide (Zirconium Corp. of America)	Minimum attack
7.	Impervious aluminum oxide (McDaniel No. AP 35)	Minimum attack
8.	Porous aluminum oxide (Norton RA 98)	Severe attack

2.1.3.2 Electrodes - The following materials were tested for possible use as electrodes:

1. Stainless steel
2. Nickel
3. Silver
4. Platinum - 10% rhodium

Of these only the platinum - 10% rhodium showed no corrosion. The rhodium is added to platinum to facilitate drawing a fine wire from which the wire gauze electrode is made.

2.2 Laboratory Tests

The first laboratory model was a cell with a 4 inch l.d. (electrolyte surface area 12.8 in^2) and a 0.25 inch thick layer of electrolyte. A ceramic coated stainless steel cell housing shown in Figure 3, was used, and the end plates were fitted with gas ports, thermocouple ports, and electrical connections. Internal support plates were made from porous aluminum oxide and heating elements were attached to these plates. The cathode was a 80 mesh, silver screen, while the anode was a .003 inch thick silver foil. A photograph of the laboratory set-up is shown in Figure 4 and a flowsheet of the process in Figure 5.

2.2.1 Test No. 1

The assembled and insulated electrochemical cell was preheated to 1000 - 1050°F over a period of approximately sixteen hours. This required a heater power of 150 to 180 watts. Carbon dioxide was fed at a rate of 0.5 SCFH at 5 psig.

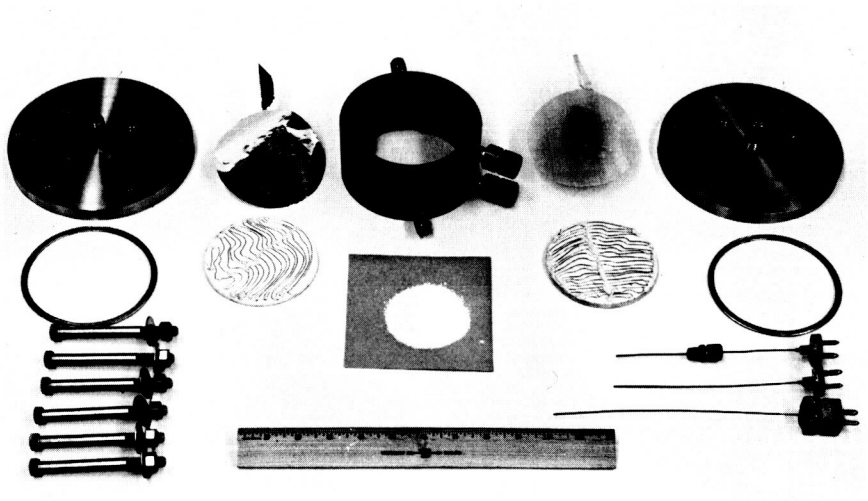

Figure 3 COMPONENTS OF ELECTROLYSIS CELL

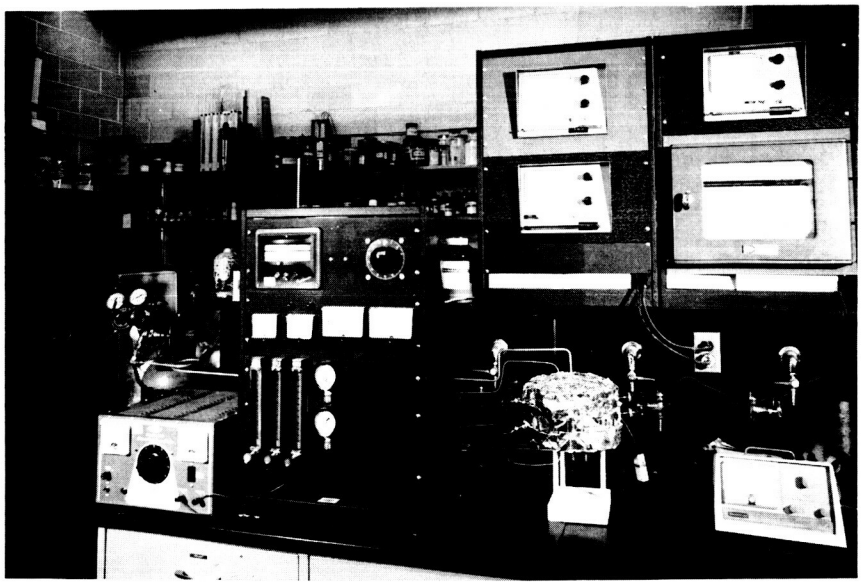

Figure 4 PHOTOGRAPH OF ELECTROLYSIS PROCESS

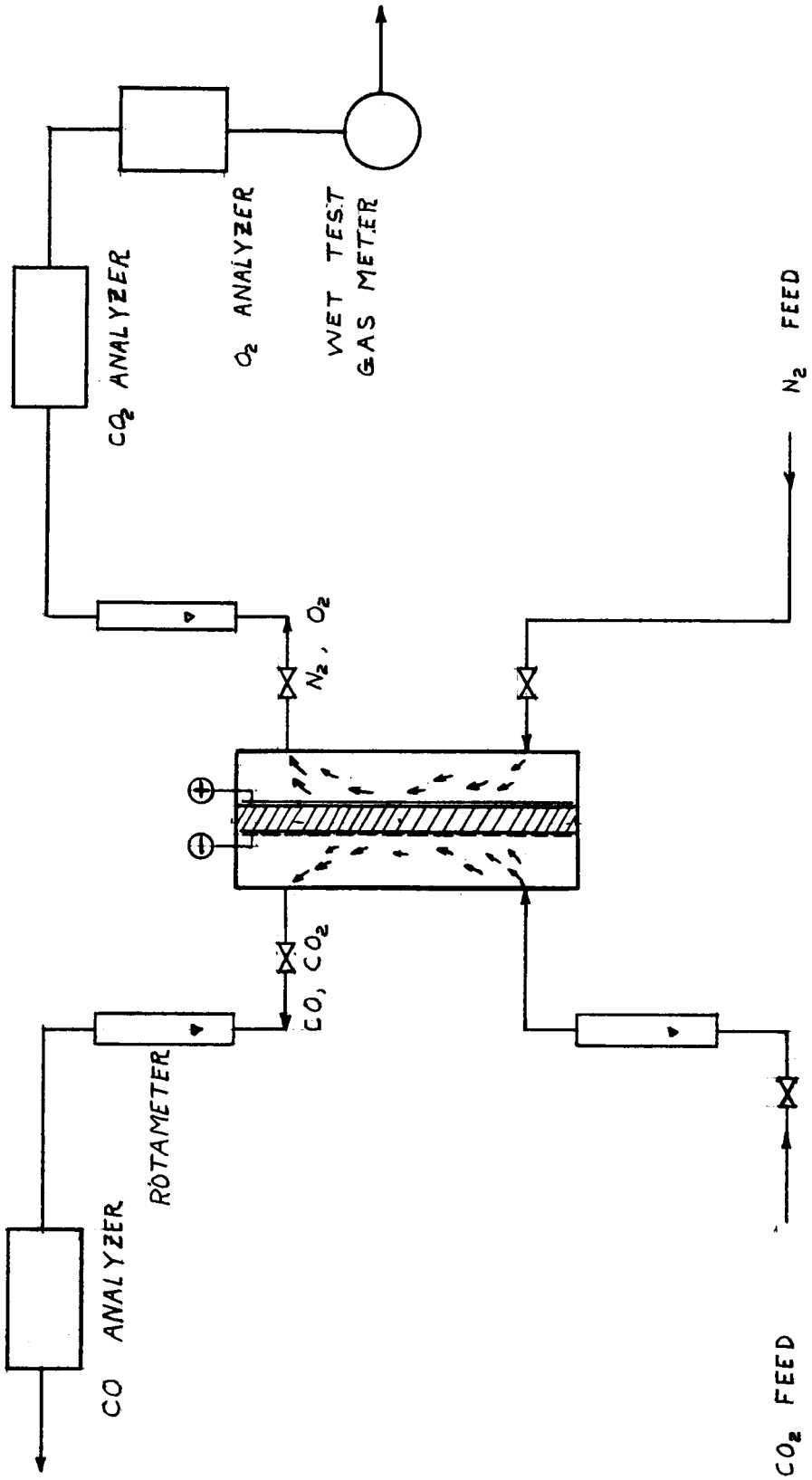

Figure 5 FLOWSHEET OF ELECTROLYSIS PROCESS

A plot of current vs. voltage across the cell is shown in Figure 6. During most of the run, the cell was operated at 2 to 3 volts.

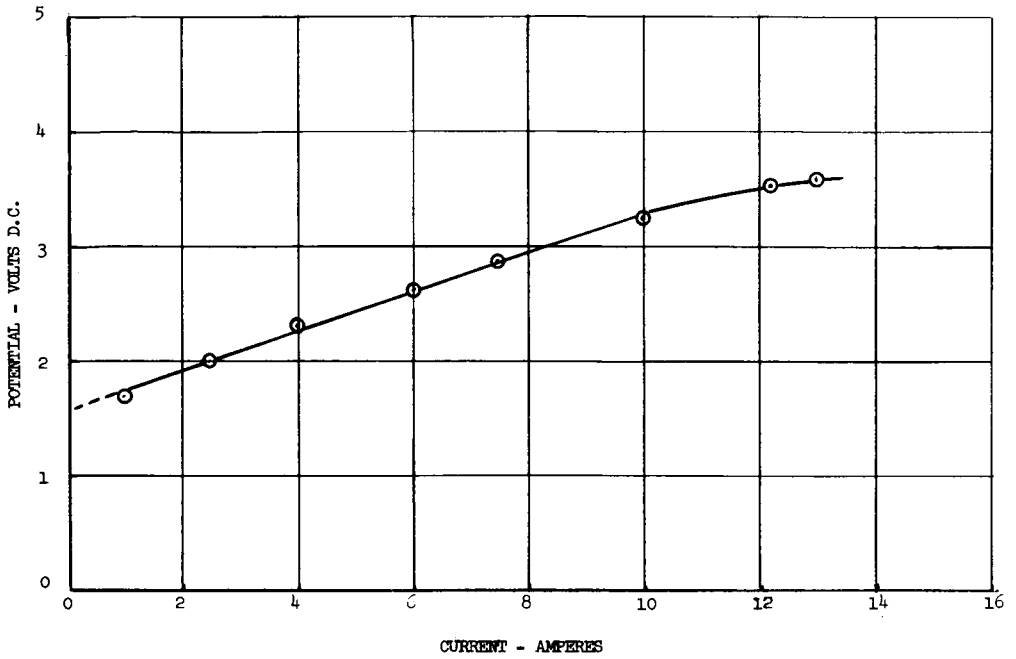

Figure 6 TEST NO. 1,
ELECTRICAL CHARACTERISTICS OF ELECTROLYSIS CELL AT 1000°F

The gas leaving the anode contained 28 - 30% oxygen (the stoichiometric amount is 33%). The cell was operated for two hours with no noticeable change in anode gas composition before it was shut down for disassembly and inspection. Upon examination after the cell was taken apart, the silver foil anode appeared to have separated from the cell housing. This allowed CO_2 to enter the anode gas stream. An oxygen concentration below 33% indicated leakage across the electrolyte.

As shown previously in the equilibrium curves in Figure 2, operation at 1000°F should produce carbon on the cathode. Figure 7 shows the buildup of carbon over the silver screen cathode. This layer was approximately 1/8 inch thick and encased the cathode. The electrolyte matrix was removed from the cell to see if the carbon was deposited only at the cathode or throughout the matrix. A carbon deposit throughout the electrolyte could indicate a decomposition of the matrix. As shown in Figure 8, after the matrix was broken open, the carbon had deposited only at the cathode surface. This indicated that the carbon resulted from decomposition of the feed CO_2 gas, rather than from the carbonate matrix.

2.2.2 Test No. 2

Test No. 2 was a rerun of Test No. 1 except the operating temperature was increased to 1300°F. After operating for 5 minutes the silver foil anode ruptured as evidenced by a rapid rise in the anode exit gas flow. The anode gas contained 92% CO_2 indicating leakage across the electrolyte. Also current leaked through the ceramic glaze to the steel cell housing. Subsequent experiments showed that at 1300°F the ceramic glaze loses its electrical insulating properties. This run was ended after 2 hours due to both the gas and electrical leaks.

2.2.3 Test No. 3

A nitrogen purge line was attached to the anode gas manifold of the electrolysis cell in this test. The purpose of flushing the anode with nitrogen was to balance the pressure across the cell and thereby prevent rupturing the silver foil anode. All other parameters remained the same as for Test No. 2.

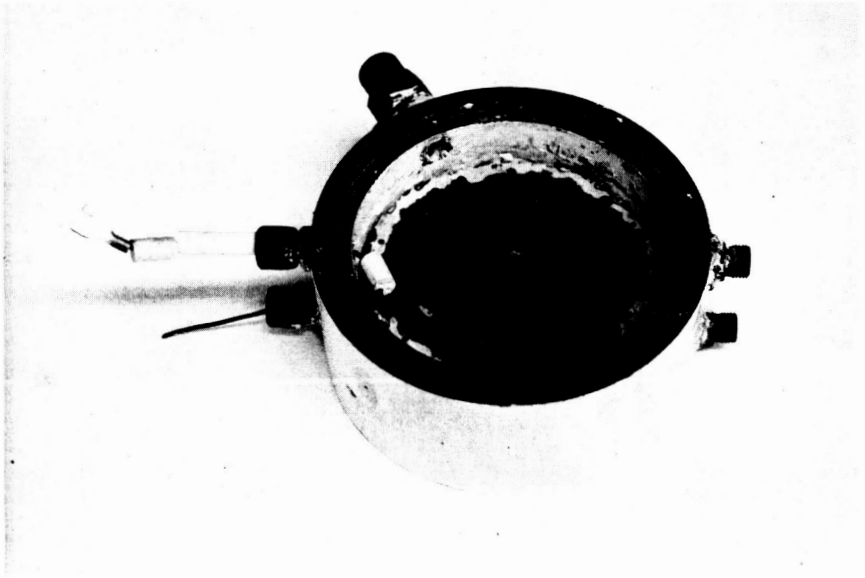

Figure 7 TEST NO. 1
CARBON COVERED CATHODE. END PLATE,
HEATER, AND SUPPORT PLATE REMOVED

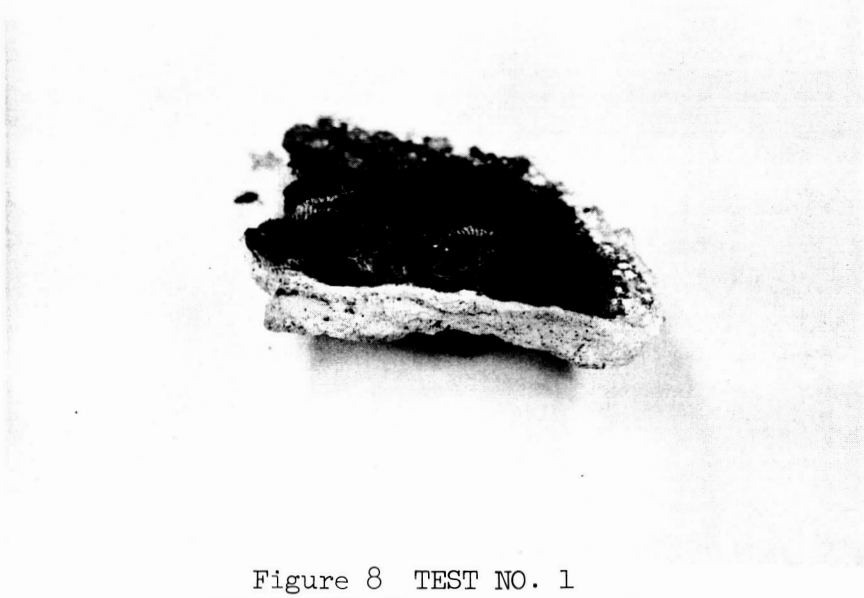

Figure 8 TEST NO. 1
CARBON DEPOSIT ON CATHODE AND SURFACE OF ELECTROLYTE

In spite of the addition of the nitrogen purge, carbon dioxide leaked across the electrolyte and very little oxygen was detected. After the run was ended, the silver foil anode was examined under the microscope and found to be full of small pinholes. Subsequent corrosion tests proved that silver cannot be used for the anode, since it is attacked by the carbonate electrolyte, particularly when acting as a positively charged electrode.

2.2.4 Test No. 4

This test was similar to test No. 3 except 80 mesh platinum - 10% rhodium electrodes were substituted for both silver electrodes; this material is not attacked by the carbonate electrolyte. The nitrogen purge was again used and the operating temperature was 1300°F. The run lasted for 29 hours and was ended because of gas leakage across the electrolyte and electrical leakage across the ceramic insulation. The anode gas contained only 2% oxygen, but over 32% carbon dioxide with the remainder being nitrogen. The cathode exit gas contained only 2% carbon monoxide, with the remainder assumed to be carbon dioxide. Based on feed and purge flow rates of 0.1 SCFH these concentrations indicated definite cross-leakage. After the cell was taken apart, the electrolyte was found to have pulled away from the cell housing, forming a path for gas leakage.

2.2.5 Test No. 5

In this test the magnesium oxide content of the electrolyte was decreased from 50 percent by weight to 34 percent. This was done to decrease the viscosity of the molten electrolyte and thereby help to prevent gas leakage across the electrolyte. However, the electrolyte was still not fluid enough to prevent leakage. When the cell was disassembled, several bolts were found broken; there was probably additional leakage to the outside of the cell.

2.2.6 Test 6

This test used a cell housing machined from boron nitride for the purpose of eliminating the electrical short circuiting which occurs after failure of the ceramic coating on the stainless steel housing. Also the magnesium oxide content of the electrolyte was reduced to 31 percent to further reduce the electrolyte viscosity. Both electrodes again were 80 mesh platinum - 10% rhodium wire gauze and the cell diameter was changed from 4.0 inches to 3.5 inches. This reduced the cross sectional area to 0.067 ft^2. The thickness of the electrolyte was increased from 0.25 inches to 0.5 inches.

After the cell was heated to 1300°F the D.C. power for electrolysis was turned on. The voltage varied from 1 to 2 volts and the current varied from 2 to 3 amps. Carbon dioxide was fed to the cathode at 0.15 CFH and nitrogen was purged through the anode at 0.1 CFH. No exit flow was detected so an aspirator was connected to the anode and cathode outlets. The effluent cathode gas contained up to 15 percent CO but most of the time it was about 5 percent. The effluent cathode gas contained up to 24 percent oxygen and up to 68 percent carbon dioxide; however, the material and electric inputs and outputs did not balance so gas leakage from outside the cell was suspected.

After the run was ended and the cell disassembled, a large number of cracks were found in the boron nitride cell housing. The different rates of thermal expansion of the stainless steel end plates and the boron nitride housing probably caused the mechanical failure. Also, when the cell was taken apart, a large build-up of carbon was found on the cathode and in the electrolyte. Figure 9 shows the carbon distributed over the cathode surface. The ceramic support in the left of the photograph has been removed from the cathode surface of the electrolyte; some of the cathode mesh and a small amount of the white electrolyte adhered to the lower half of the support. Figure 10 shows the depth of penetration of carbon extending from

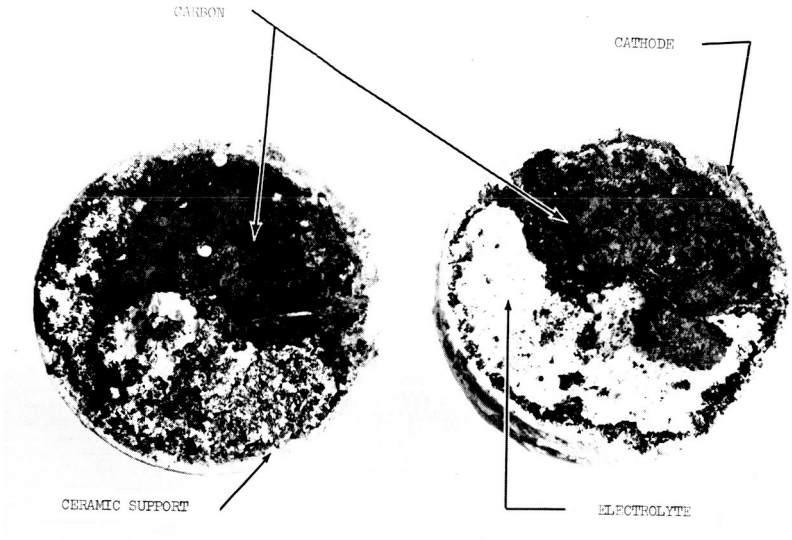

Figure 9 TEST NO. 6
CARBON FORMATION ON CATHODE

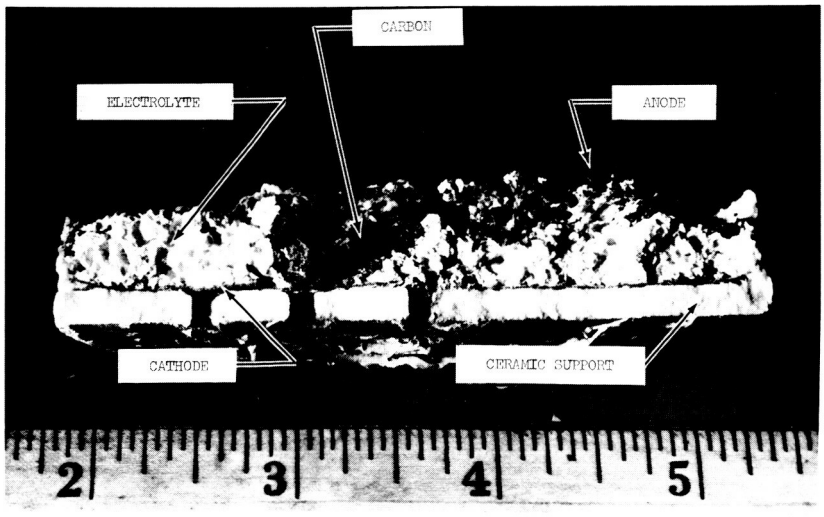

Figure 10 CARBON BUILD-UP WITHIN ELECTROLYTE

the cathode through the electrolyte to the anode. This occurred even though the operating temperature was 1300°F, which is considered to be sufficiently high to minimize the formation of carbon. This carbon in the electrolyte appeared to come from physical buildup of carbon at the cathode which then forced its way through the semi-solid electrolyte. This was the last test with the flat plate design.

2.3 Other Configurations

Two alternate design approaches were evaluated in an attempt to overcome leakage due to thermal expansion of component parts of the cell, leakage due to insufficient sealing between the electrolyte and the cell housing, and electrical short circuiting. The first was to impregnate a porous alundum tube with molten carbonates. This proved unsatisfactory for two reasons: (1) the molten carbonate exudes out of the pores, leaving paths for gas leakage and, (2) the molten carbonate severely attacked the porous aluminum oxide at elevated temperatures causing the tube to lose its structural strength.

The other approach considered was to coat a tubular shaped wire gauze electrode with a layer of electrolyte. In this method the electrolyte would have to be self supporting between two electrodes. The electrolyte could be applied in the molten state; however, when the assembly was cooled to room temperature, the electrolyte solidified, cracked, and then peeled away from the electrode. Thermal contraction was the cause of the cracking and subsequent peeling. These two approaches then were eliminated from further consideration.

Due to increased emphasis on the fabrication and operating of the catalytic reactor for carbon monoxide disproportionation, no additional investigation was conducted on the carbonate electrolysis cell.

2.4 Conclusion

The principles and concepts of using a high temperature carbonate electrochemical cell to reduce carbon dioxide to carbon monoxide and oxygen were verified in several cells which were constructed and operated. The problems which remain to be solved before this system becomes operational are:

1. Obtaining materials of construction which withstand the attack of the carbonates over a long period of time.
2. Preventing the formation of carbon on the anode (Operation at higher temperatures favor the formation of carbon monoxide).
3. Obtaining gas-tight seals between the cell support and the electrolyte.

SECTION 3

THE SELECTIVE PERMEATION OF OXYGEN THROUGH SILVER

3.1 Background

Silver and certain silver alloys have the unique property of being selectively permeated by oxygen; that is, silver acts as a membrane which allows only the passage of oxygen and holds back all other gases. This is similar to the phenomena of hydrogen diffusion through palladium and palladium alloys.

The phenomenon is not completely understood; however, the following mechanisms are believed to take place in the diffusion process.

1. Oxygen gas dissolves in the metal.
2. Molecular oxygen dissociates into atomic oxygen.
3. The atoms pass through the interstitial sites of the crystal lattice rather than along grain boundaries.
4. The atoms recombine to form molecules and leave the surface of the membrane.
5. The driving force is a gradient of the partial pressure of oxygen and is proportional to $(P)^{1/2}$.

An equation for the rate of oxygen diffusion can be written as:

$$Q = \frac{KA}{t}(P_1^{1/2} - P_2^{1/2})e^{-E/2RT}$$

where Q is the rate of gas diffusion, (cm^3/hr STP)

K is a diffusion constant which is dependent upon the gas-metal (alloy) system

A is the area of the membrane (cm^2)

t is the thickness of the membrane (cm)

P_1 is the partial pressure of the permeating gas on the feed stream side (mm Hg)

P_2 is the partial pressure of the permeated gas on the low pressure side (mm Hg)

e is the base of natural logarithms

E/2 is the energy of diffusion (gram calories per gram-atom)

R is the gas constant

T is the absolute temperature (°K).

From this equation, it is apparent that the rate of permeation can be increased by decreasing the thickness of the membrane, increasing the oxygen pressure differential, and by increasing the temperature. These parameters can be varied within the following limits.

1. The rate of diffusion is fixed by the design capacity of the system, i.e., the number of men.
2. Minimum membrane thickness at the present time appears to be approximately 0.025 mm (.001") for flat stock and 0.125 mm (.005") for tubes.
3. P_1 is determined by the inlet total pressure, composition, and feed rate.
4. P_2 is determined by the downstream total pressure, and diluent flow rate, if a gas such as nitrogen is used to flush this side of the membrane.

5. The total pressure differential is limited by the strength of the membrane and/or membrane support at the operating temperature.

6. The limiting temperature is that which approaches the melting point of the membrane of brazing alloys (if any) used in construction.

The most serious difficulty with this process is the formation of pinholes along the grain boundaries of the membrane. These holes appear after continuous operation at elevated temperatures, and appear to be related to grain growth and an accompanying increase in size of the grain boundary. Some materials deteriorate within a day while others have been operated continuously for several months before failing.

3.2 Experiments and Results

The experiments were divided into two types, namely, (1) determination of materials which would withstand the operating conditions without premature failure, and (2) operation of a cell to determine permeation rates.

3.2.1 Material Selection

Original tests were conducted with the membrane used as the anode in the molten carbonate electrolytic cell. This would have had the advantage of increasing the rate of oxygen diffusion because as soon as oxygen atoms were formed in the electrolytic reaction, they could have started to diffuse through the membrane. Unfortunately the silver was severely attacked. The reaction which probably took place was:

$$2\ Ag + CO_3^{=} \longrightarrow Ag_2CO_3 + 2e^- \qquad E^\circ\ -0.47\ v$$

Photomicrographs of typical pinholes which were formed are shown in Figures 11 and 12.

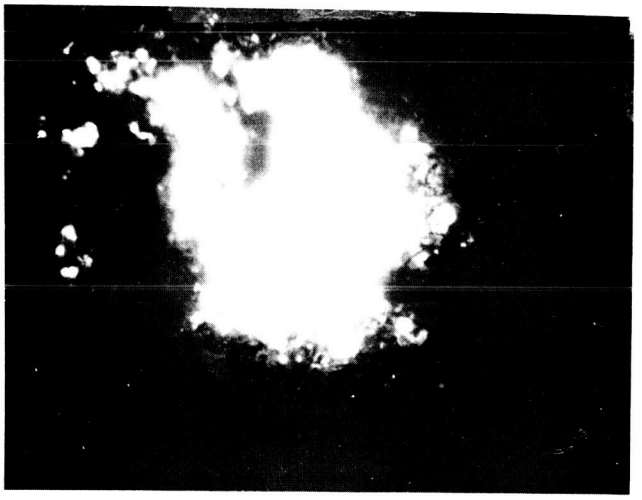

Figure 11 HOLE FROM ELECTROLYTIC CORROSION IN SILVER ELECTRODE (150X)

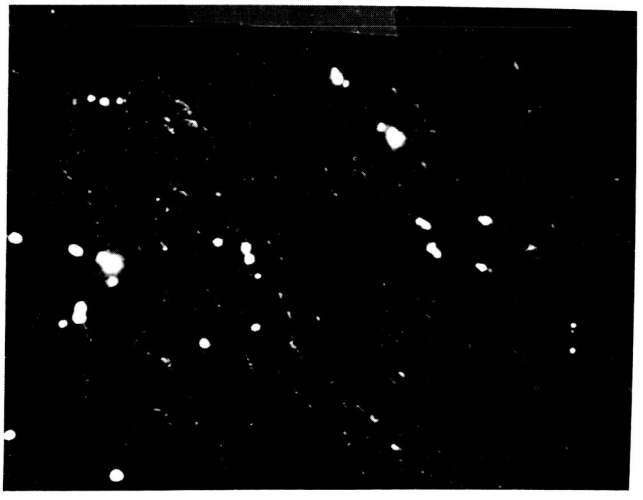

Figure 12 PINHOLES IN SILVER ELECTRODE (150X)

Next a silver membrane was tested as an oxygen diffusion membrane without being in contact with the carbonate electrolyte and without serving as an electrode. The membrane was a tube made from 99.99% pure silver, 5.5" long x 0.4" diameter, with a 0.004" wall. A feed gas manifold and end cap were silver brazed to the tube. The assembly was tested at room temperature at 15 psig internal pressure and was found to be free from leaks.

Next, the cell was slowly heated from room temperature to 1300°F over a period of 3 days. Nitrogen was used to pressurize the inside of the silver tube to 2" H_2O. The cell did not leak when left overnight in this condition. The nitrogen pressure then was increased to one psig and a large volume of gas came through the silver tube. The unit was shut down, disassembled, and inspected. A large number of microscopic pin holes were found in the silver tube; also, the surface of the silver had a crystalline grainlike appearance. This indicated that either corrosion or changes in crystal structure were probably responsible for the leaks.

Microscopic examination showed large grain growth when the material was compared to a tube which had not been heated (Figures 13 and 14); the majority of the pinholes were found along grain boundaries. A search was undertaken which included examining existing literature and contacting precious metal fabricators to find a method for controlling grain growth and pinhole formation. Based on the results of the search, an alloy was tested which contained 3% palladium - 97% silver, and afterwards, an alloy which contained silver with trace amounts of magnesium and nickel (alloy 15065).

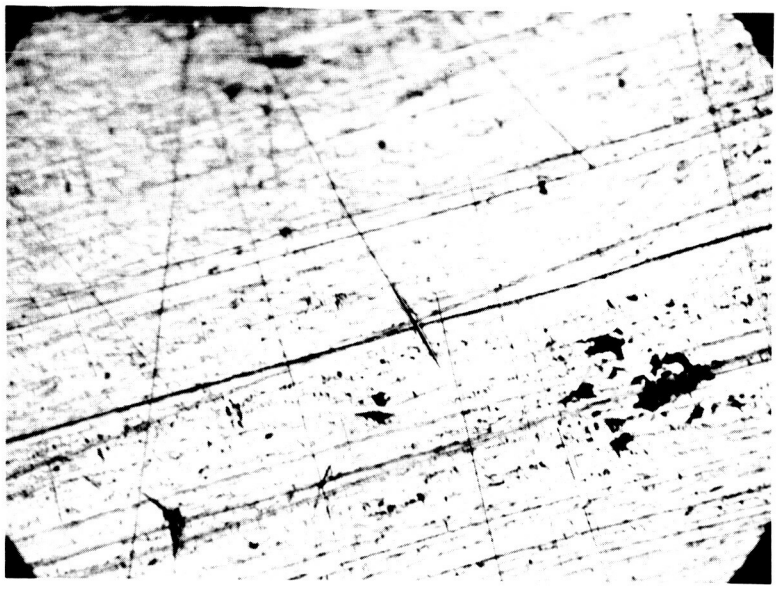

Figure 13 HIGH PURITY SILVER TUBE AS RECEIVED FROM MANUFACTURER (150X)

Figure 14 HIGH PURITY SILVER TUBE AFTER HEATING TO 1300°F, HIGH CORROSION AREA (150X)

Samples of these alloys were subjected to various combinations of gaseous atmospheres, temperature, hold time, and cooling rates in order to compare the grain growth to that of high purity silver. Photomicrographs of silver and silver alloys after undergoing tests are shown in Figures 15 through 24.

Since neither the silver-palladium alloy nor the silver-trace Mg-Ni alloy showed the large grain growth that high purity silver exhibits, tubes were fabricated from these alloys.

3.2.2 Test Procedure

The flow sheet in Figure 25 shows the laboratory set-up which was used to test the oxygen diffusion concept and to obtain rates of oxygen permeation with varied parameters. The feed gas flow was measured with a rotameter; the gas was fed through a tube to the bottom of the diffusion tube, along the walls of the tube, and out through a port at the top of the cell. A valve (1) in the feed gas exit line controlled the internal pressure. The manifold (downstream) side of the diffusion cell was flushed with nitrogen, to control the oxygen partial pressure during long duration continuous runs. Nitrogen fed to the top of the manifold, passed along the exterior wall of the diffusion cell and left the manifold. In tests where nitrogen was not used, exit gas collected in a gas burette to measure the increase in gas volume as a function of time (valve 2 closed, valve 3 open). When continuous runs were conducted with a nitrogen flush, the gas exited through valve 2 (valve 3 closed) and samples were taken and analyzed with a gas chromatograph. The rate of oxygen permeation was determined from nitrogen flow rate plus gas analysis data.

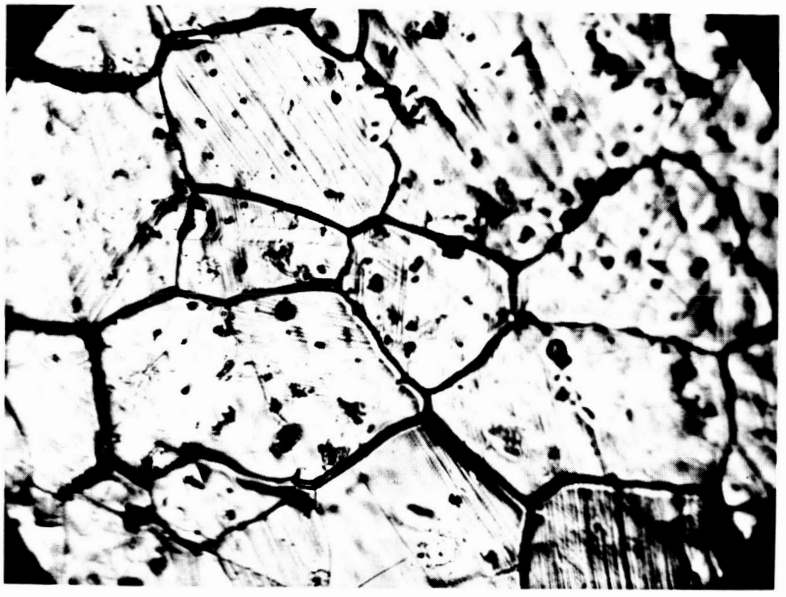

Figure 15 HIGH PURITY SILVER TUBE AFTER HEATING TO 1300°F, LOW CORROSION AREA (150X)

Figure 16 HIGH PURITY SILVER TUBE PLACED IN 1300° F FURNACE FOR 2 HOURS, FOLLOWED BY WATER QUENCH (150X)

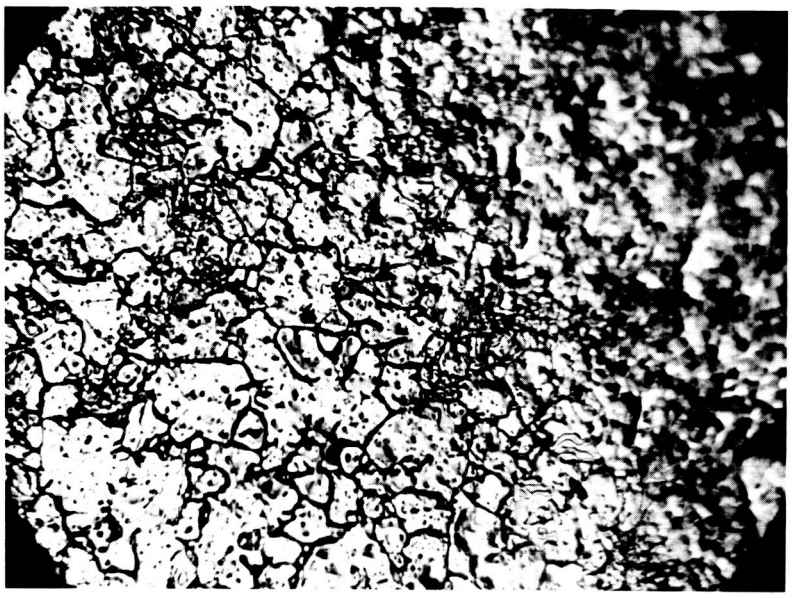

Figure 17 HIGH PURITY SILVER TUBE PLACED IN 1300°F FURNACE FOR 21 HOURS, THEN COOLED IN AIR (150X)

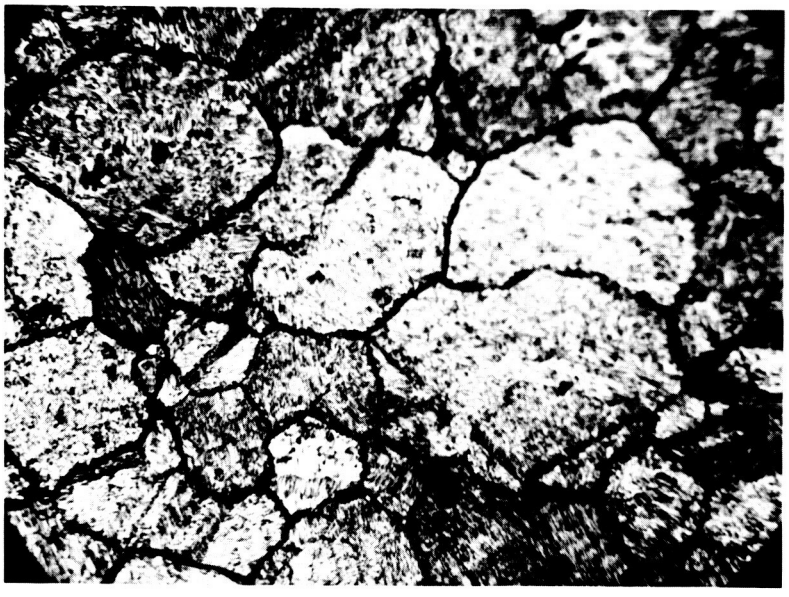

Figure 18 HIGH PURITY SILVER TUBE SLOWLY HEATED TO 1300°F, HELD AT 1300°F FOR 40-1/2 HOURS, FURNACE COOLED (150X)

Figure 19 HIGH PURITY SILVER TUBE PLACED IN 1300°F FURNACE FOR 89 HOURS UNDER NITROGEN ATMOSPHERE - FURNACE COOLED (150X)

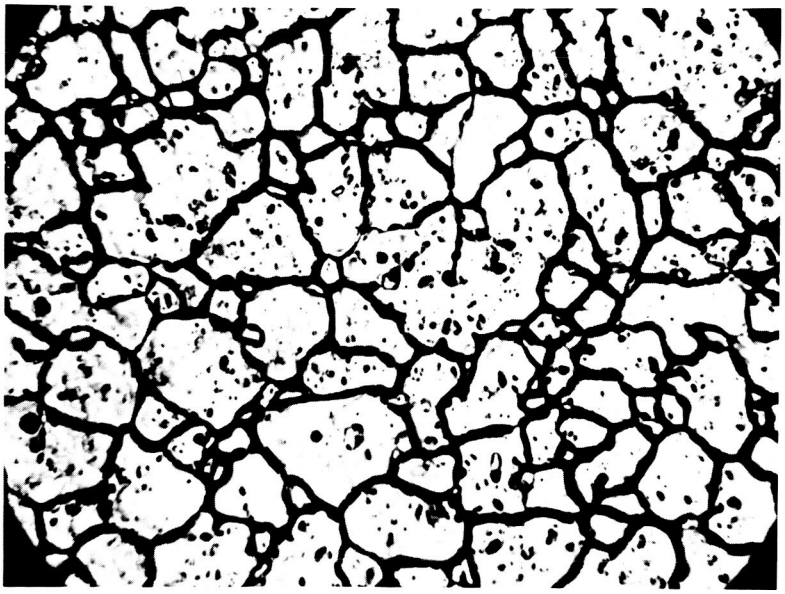

Figure 20 HIGH PURITY SILVER TUBE PLACED IN 1300°F FURNACE FOR 89 HOURS UNDER NITROGEN ATMOSPHERE - WATER QUENCH (150X)

Figure 21 ALLOY OF 3% PALLADIUM-BALANCE SILVER AS RECEIVED FROM MANUFACTURER (150X)

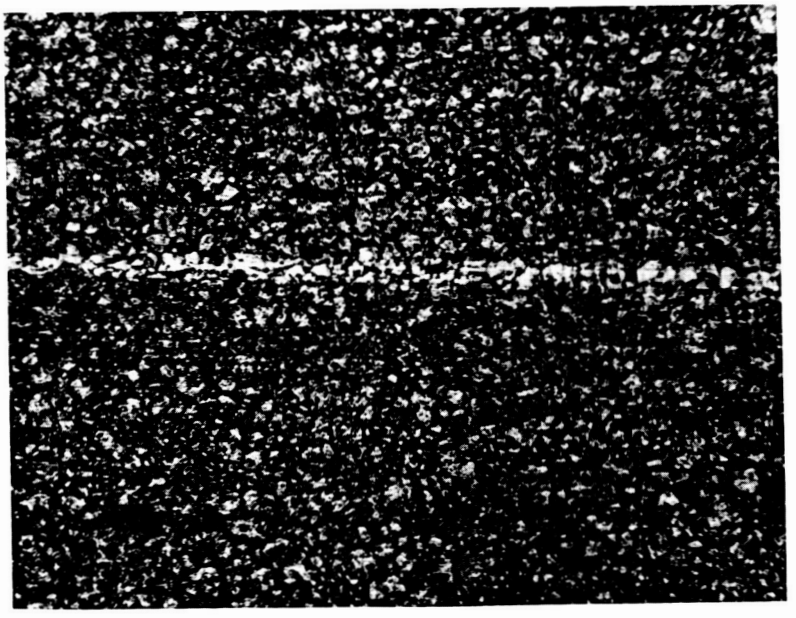

Figure 22 ALLOY OF 3% Pd-BALANCE SILVER PLACED IN 1250° - 1430°F FURNACE FOR 165 HOURS FOLLOWED BY WATER QUENCH (150X)

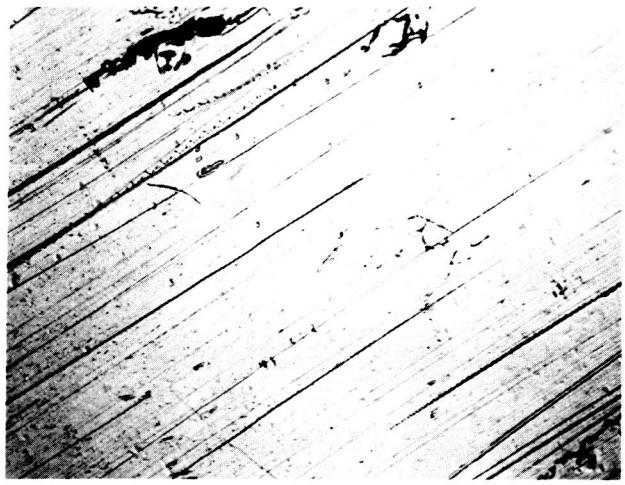

Figure 23 ALLOY 15065 AS RECEIVED FROM MANUFACTURER (150X)

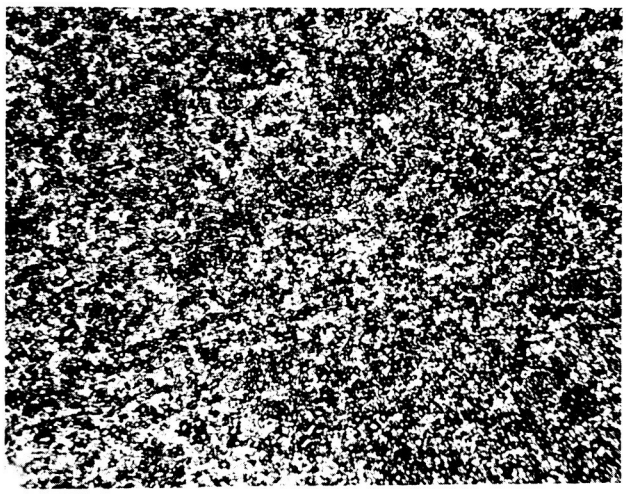

Figure 24 ALLOY 15065 PLACED IN 1250°F FURNACE FOR 11¼ HOURS FOLLOWED BY WATER QUENCH (150X)

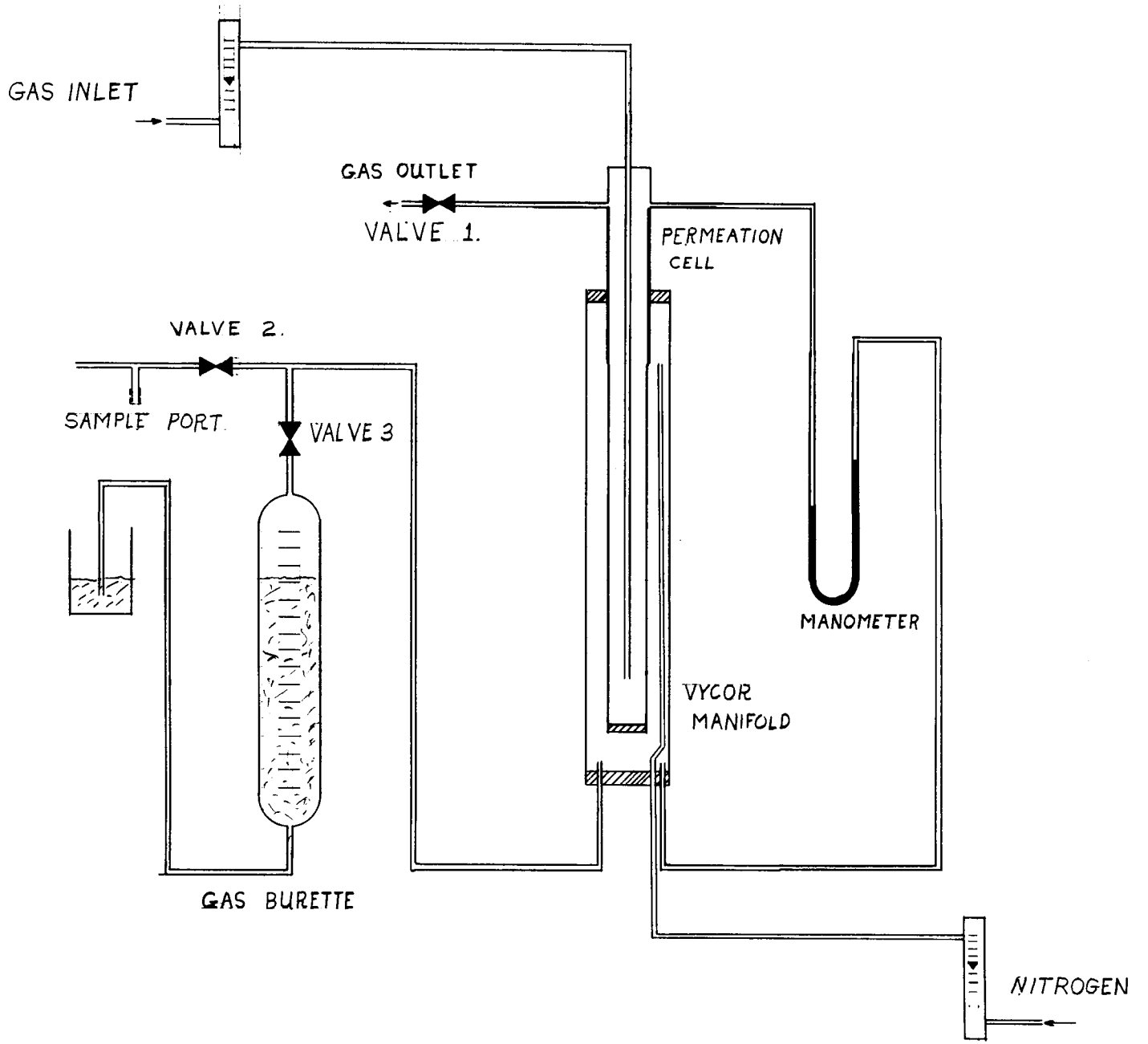

Figure 25 SCHEMATIC DIAGRAM OF OXYGEN PERMEATION TEST ASSEMBLY

The permeation tube, as shown in Figure 26, consisted of a silver alloy tube with a silver plug brazed on one end and a stainless manifold on the other end. The cell made from the alloy 3% Pd - 97% Ag consisted of a tube 12" long x 0.4 " dia x 0.005" wall, the cell made from alloy 15065 consisted of a tube 12" long x 015" dia x 0.0085" wall. A photograph of the cell inside of the 1.0" o.d. x 18" long Vycor tube is shown in Figure 27. Also shown are the thermocouples used to indicate the wall temperature of the silver alloy cell. The Vycor manifold fits inside a cylindrical electric heater which is covered with thermal insulation.

3.2.3 Results

Oxygen permeation through the 3% palladium - 97% silver alloy tube, which is described in Section 3.2.2, was not detectable under the following conditions:

1.	Temperature	900° - 1330°F
2.	Feed gas	99.8% oxygen
3.	Manifold gas	99.99% nitrogen

This tube was operated for three weeks before a leak developed at one end of the silver solder joints. A spare tube was operated for five days before failure. Again no permeation was detected. After another leak developed the run was terminated.

A new assembly, as described in Section 3.2.2, was constructed from silver alloy 15065. This tube was operated without failure for two months and the rate of oxygen permeation was greater than the literature values for pure silver. During the run, leak checks were performed periodically to confirm

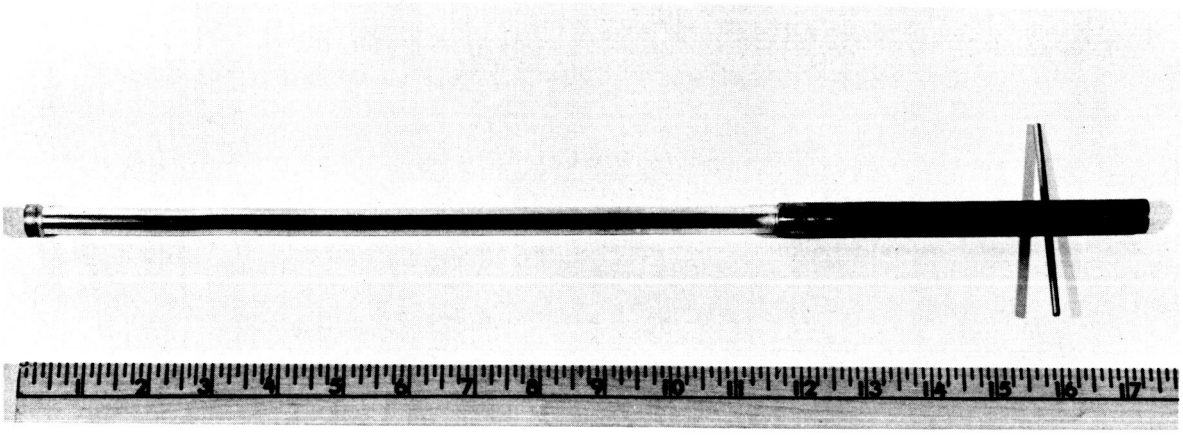

Figure 26 SILVER ALLOY PERMEATION TUBE WITH END CAP AND FEED GAS MANIFOLD

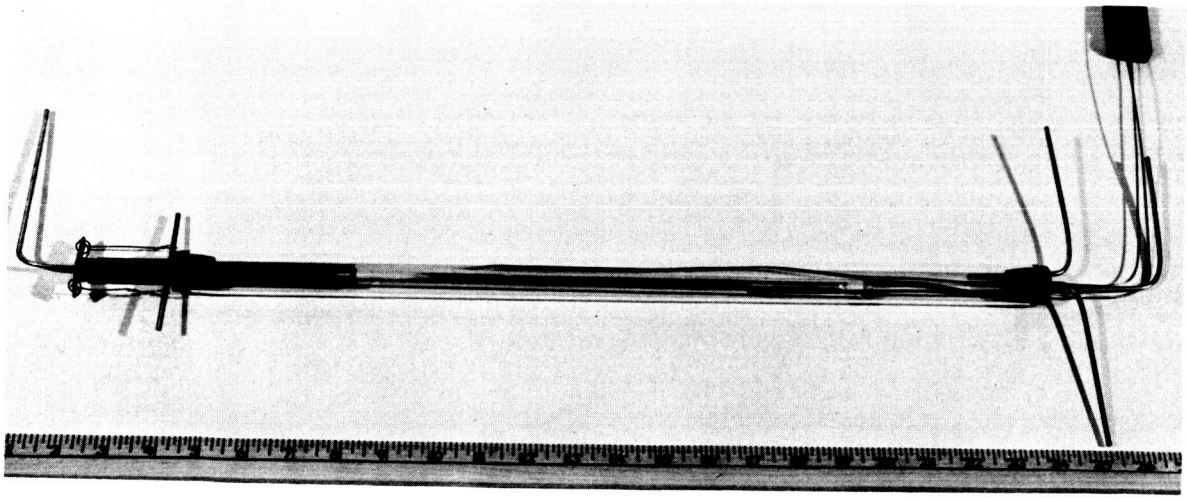

Figure 27 PERMEATION TUBE ASSEMBLED INSIDE OF VYCOR MANIFOLD
WITH GAS DELIVERY TUBES AND THERMOCOUPLES

that the oxygen flow was by diffusion and not leakage. This was accomplished by flushing both sides of the membrane with nitrogen, applying a pressure differential and observing if there was any decrease in pressure on the high pressure side.

The temperature of operation and the feed gas composition were varied during the run in order to obtain design information. The two feed gas compositions were 99.8% pure oxygen and a mixture containing 33.2% oxygen - 66.8% carbon dioxide; the temperature was varied from 1300° to 1400°F, the high limit of operation determined by the melting point of the silver brazing alloy used in the construction of the cell. The rates of oxygen permeation are shown in Table 4. The rates of permeation with the test cell are greater than those published by other researchers. This is attributed to the use of an alloy of silver instead of pure silver. The same phenomenon is known to take place in the hydrogen-palladium system; i.e., certain alloys of palladium allow greater rates of hydrogen permeation than pure palladium.

After two months of continuous operation a leak was suspected when a trace of carbon dioxide from the feed gas appeared in the gas stream of permeated oxygen and nitrogen. The cell was turned off and disassembled, and the silver alloy tube was pressurized with air and placed in a water bath. A large number of extremely small leaks were found over the entire surface of the silver alloy tube. Subsequent microscopic examination confirmed that cracks had developed along the grain boundaries of the alloy. Photomicrographs of the surface after the 2 month run are shown in Figures 28 and 29.

Table 4 OXYGEN PERMEATION RATE

Temp. Range °F	Vol. % Oxygen	Experiemntal Permeation Rate $cm^3/hr.$	Calculated From (1)	(2)
1300 - 1310	99.8	20.4 - 29.4	16.9	16.1
1350 - 1370	99.8	29.4 - 45.0	24.4	22.8
1300 - 1310	33.2	10.2 - 13.8	9.7	9.2
1350 - 1360	33.2	24.6 - 28.0	14.0	13.1
1380 - 1390	33.2	30.1	16.5	15.5

1. Cole, R. E., THE PERMEABILITY OF SILVER TO OXYGEN, Brit. J. Appl. Phys. 1963, Vol. 14

2. Johnson, F. and Larose, P., THE DIFFUSION OF OXYGEN THROUGH SILVER, J. Am. Chem. Soc. 1924, Vol. 46

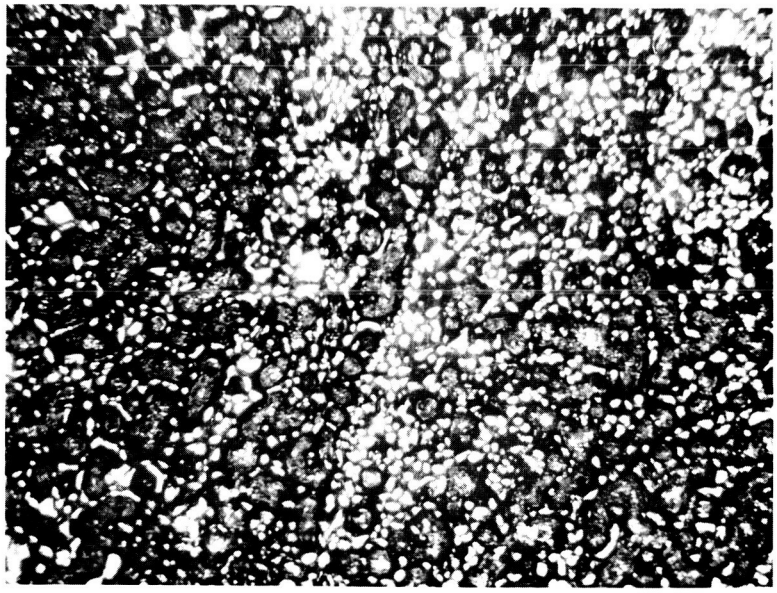

Figure 28 SILVER ALLOY 15065 AFTER 2 MONTHS OPERATION
IN THE TEMPERATURE RANGE 1300° - 1400°F
AREA 1 (150X)

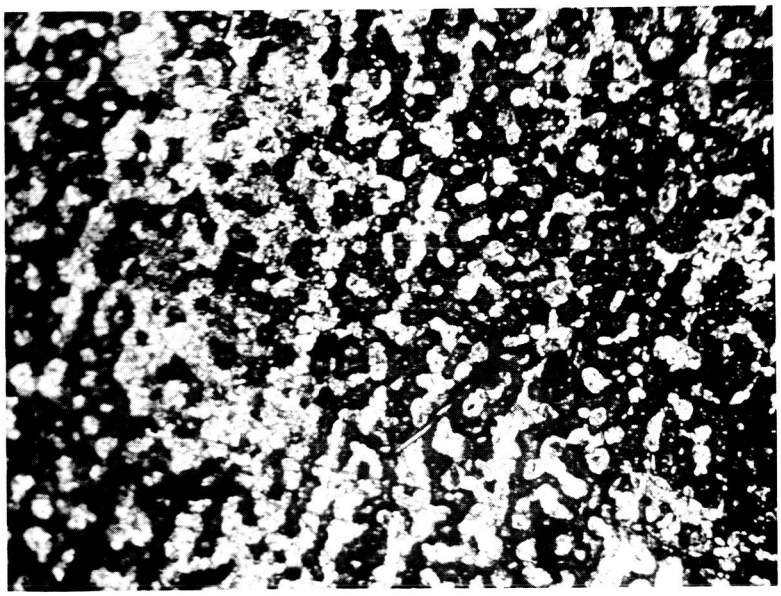

Figure 29 SILVER ALLOY 15065 AFTER 2 MONTHS OPERATION
IN THE TEMPERATURE RANGE 1300° - 1400°F
AREA 2 (150X)

3.3 Conclusion

The separation of oxygen from carbon dioxide was achieved on a continuous basis over an extended period of time. The use of a silver alloy which contains trace quantities of nickel and magnesium yielded higher rates of permeation than the reported results for pure silver. The rate of permeation can be further improved by (1) the use of membranes with thinner walls, (2) operation at a higher temperature, and (3) development of more effective alloys.

The wall thickness of tubes fabricated from this alloy can probably be decreased as more experience with this alloy is obtained. The temperature during the tests was limited to 1400°F because of the melting point of the brazing alloy which was used; however, if the necessary fittings had been welded, the operating temperature could have been increased to values approaching the melting point of silver (1760°F).

The problem of increasing the operating life requires the development of an improved silver alloy, which may also increase the rate of permeation. This phenomenon was observed in the improvement of both operating life and permeation rate when alloy 15065 was substituted for pure silver.

SECTION 4

CATALYTIC DISPROPORTIONATION OF CARBON MONOXIDE

The equilibrium of the reaction 2 CO $\rightarrow$ CO_2 + C is dependent upon temperature as shown in Figure 30; however, the rate of reaction is extremely slow unless a suitable catalyst is present. Materials which are known to function as catalysts for this reaction include nickel, iron and cobalt. The primary phases of investigation of this process consisted of (1) a literature survey reviewing the present state of the art, (2) catalyst evaluation to determine conversion efficiencies and carbon to catalyst ratios under various parameters, and (3) design, construction, and operation of a prototype reactor (Section 5).

4.1 Parameters

The variables which were tested during this program included:

(1) Feed gas CO:CO_2 ratios: 1:0, 1:1, 1:9, by volume

(2) Temperature 600 - 1600°F

(3) Catalyst form: granules, strips, felt, and wool, plus powders supported on alumina or quartz wool.

(4) Flow rate: 4 - 50 std Cm^3(STP) per min cm^2

(5) Pressure: 1 atmosphere

The specific objectives were to achieve maximum CO conversion, and high weight ratio of carbon formed to catalyst required.

4.2 Laboratory Set-Up

The flow sheet in Figure 31 and the photograph in Figure 32 show the laboratory set-up which was used for evaluation of catalysts.

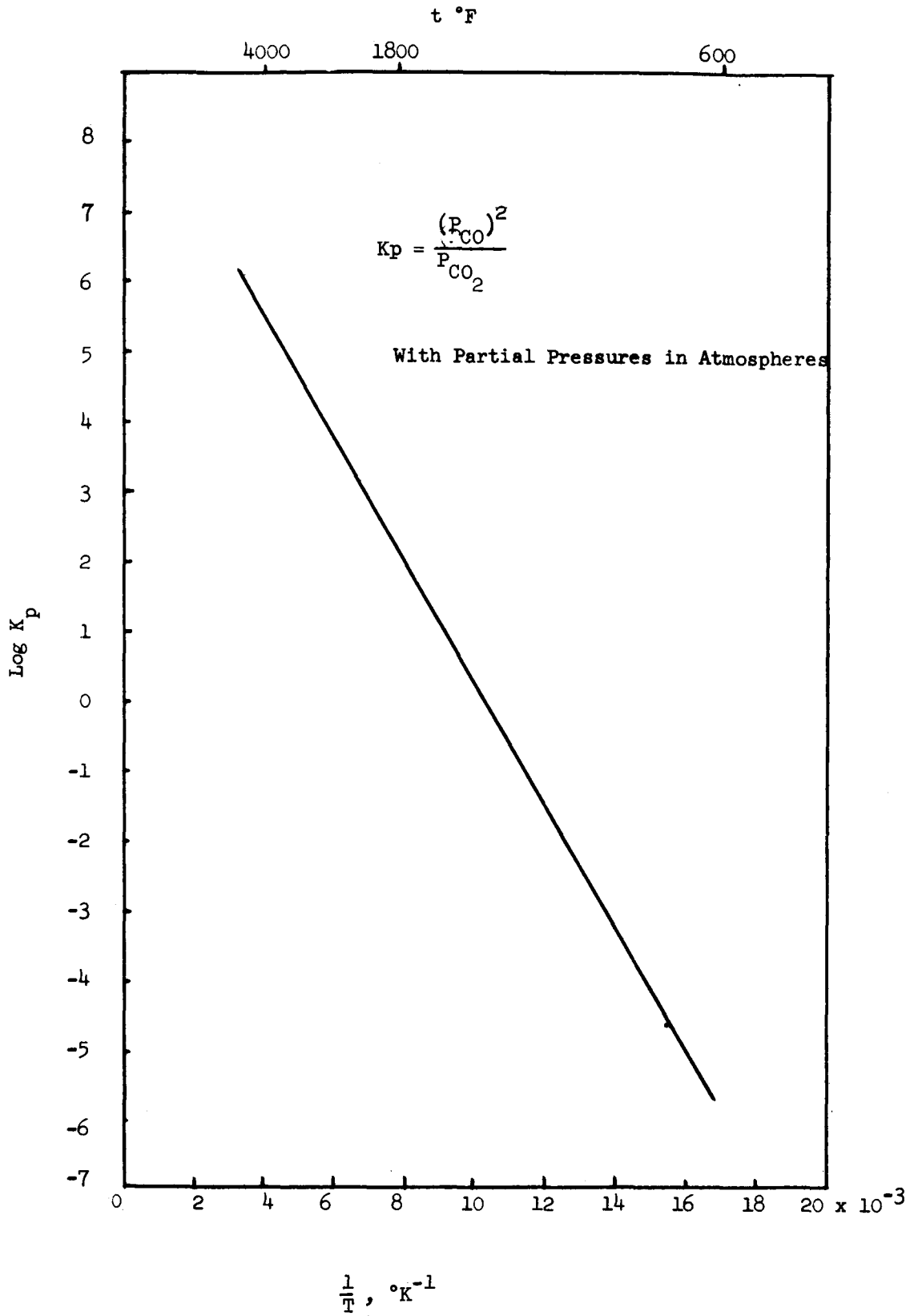

Figure 30 EQUILIBRIUM FOR THE REACTION C + CO_2 → 2CO AS A FUNCTION OF TEMPERATURE

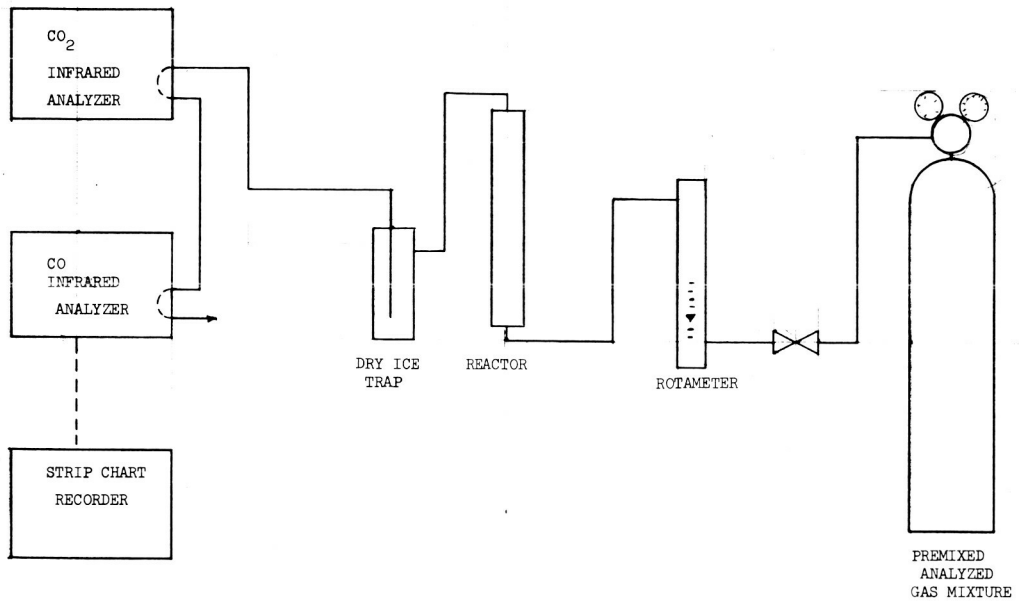

Figure 31 SCHEMATIC DIAGRAM OF LABORATORY CATALYSIS EXPERIMENTS

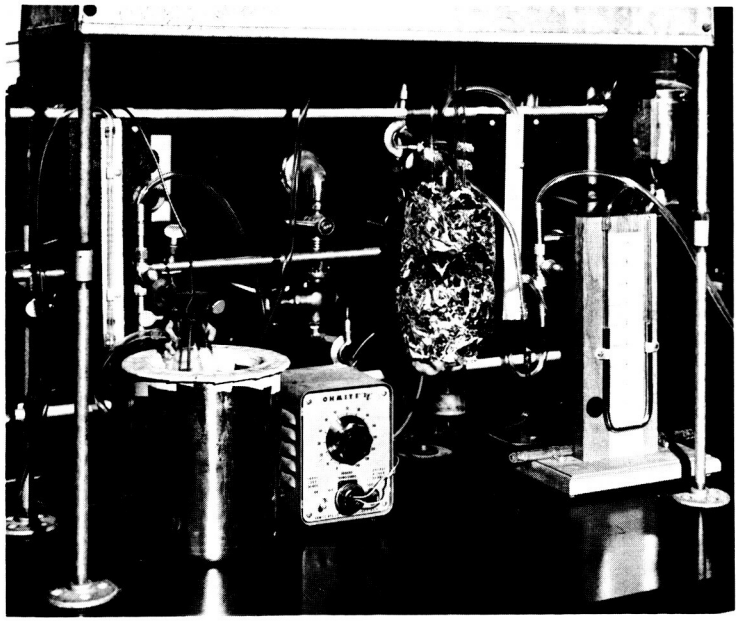

Figure 32 PHOTOGRAPH OF LABORATORY CATALYSIS APPARATUS

The gas mixture was fed from a pre-mixed, analyzed gas cylinder, through a needle valve and rotameter to the reactor. The gas stream leaving the reactor passed through a dry-ice trap and then to continuous infrared analyzers for measurement of carbon monoxide and carbon dioxide concentrations. A dry-ice trap was needed for removal of nickel carbonyl which formed when some types of nickel were being evaluated at lower temperature; the carbonyl interfered with readings on the CO analyzer. The formation of carbonyls was not detected at temperatures near 1000°F; the presence of carbonyls is undesirable since they are extremely toxic.

4.2 Forms of Catalysts

4.3.1 Pellets

The original form of catalyst tested was 1/8" cylindrical pellets of nickel on alumina (Harshaw Ni-0707). The maximum conversion was 30 percent with 100 percent carbon monoxide feed.* When the run was ended, the pellets had expanded to several times their original size because of the internal build-up of carbon.

4.3.2 Strips

Nickel, cobalt and steel metal catalysts were tested as bundles consisting of twenty-five 2-1/2" long x 1/4" wide x 0.025" thick strips. Nickel and cobalt showed a maximum conversion of 3 percent whereas type 1018 and 1095 steels reached a conversion in the range of 50 to 60 percent with a feed gas of 100 percent carbon monoxide and a flow of 8 $cm^3/min - cm^2$. This

---

*In all of the test results described in this report, percent conversion = (amount of CO converted x 100)/(amount of CO fed).

conversion decreased as carbon formed on the surface. After the carbon was removed and fresh surface was exposed the conversion recovered to approximately 10 percent. This indicated that surface oxides formed influenced the catalytic reaction. If a flat catalytic surface could be prepared which would maintain its activity after each carbon removal process, a highly efficient system could be designed because the catalyst would be reusable.

4.3.3 Granules and Powders

The catalyst configuration used most frequently was either granular or powdered with the catalyst resting on a fine stainless steel screen. This form was easy to handle, and permitted rapid testing and comparison of a variety of catalysts.

4.3.3.1 High Surface Area Pyrophoric Powders - Several attempts were made to use high surface area metals in order to expose as much area per given weight of catalyst as possible. The first high surface area powders were made by decomposing metal formates or oxalates under an atmosphere of hydrogen, argon, or carbon dioxide. Nickel, cobalt, and iron powders were prepared by this method. Of these, nickel consistently yielded conversions greater than 90 percent with pure CO feed, although this was generally for a short time because the surface would become coated with carbon. Cobalt powder was slightly less active than nickel while iron powder yielded a maximum conversion of 70 percent. Attempts were made to obtain still greater conversion by using Raney metals. These are high porosity and high surface area metals prepared from alloys of the metals with aluminum. To activate the catalyst, the aluminum is leached with a solution of sodium hydroxide, washed, and stored

under an inert atmosphere. These catalysts are extremely pyrophoric and may explode on contact with air at room temperature. A large volume of hydrogen is adsorbed on the surface of the catalyst and this caused problems during some of the tests because as the catalyst was being heated, the hydrogen was desorbed and caused a rapid pressure rise in the reactor. This in turn blew out the end stoppers of the reactor, air entered, and the catalyst bed exploded. The maximum conversions obtained with the Raney catalysts approximated 95 percent, slightly higher than with powders prepared from decomposition of formates. However, the pyrophoric and explosive nature of Raney catalyst excluded them from further consideration for this system.

4.3.4 Felts and Wools

Nickel in the form of a felt was evaluated. This material showed little catalytic activity. Also various grades of commercial steel wool were used. These catalyst yielded conversions which were not as high as the high surface area powders, but the steel wools would maintain a high conversion for a much longer time. Cobalt was not obtained as a wool or felt and was not evaluated in this form.

The advantage of the wool form of catalyst is that the catalyst can be dispersed throughout the reactor, thereby providing space for accummulation of carbon. For some runs, a powdered catalyst was coated on quartz wool; this proved to be a satisfactory way of loading the catalytic reactor, because a high percent conversion could be obtained and the wool would prevent a rapid increase in pressure drop as the carbon was formed.

4.4 Optimum Catalyst

Of all the catalysts tested the best one for the disproportionation of carbon monoxide to carbon dioxide and carbon was found to be a nickel oxide catalyst which is manufactured by the Chemetron Corp., and is identified as Girdler H-219 nickel catalyst. This material is 100 percent nickel oxide and is used as an intermediate in the preparation of other Girdler catalysts.

4.4.1 Girdler H-219 Catalyst

The H-219 nickel oxide provided a maximum CO conversion equal to that of the high surface area powders, and operated with a lower rate of decrease in conversion. The original high conversion was attributed to a reaction between the nickel oxide and carbon monoxide which yields nickel and carbon dioxide. On completion of the reaction the elemental nickel formed acts as a catalyst for disproportionation; the activity of the nickel formed in this manner appeared greater than the other nickel catalysts which were tested. This point in time was usually indicated by a sharp fluctuation in effluent carbon dioxide concentration. Once the conversion drops to this level it holds steady or decreases slowly for a much longer period of time than for any other catalyst.

To prevent premature shut down of a run because of an excessive increase in pressure drop from carbon build-up, the catalyst was dispersed in the reactor by (1) using a multi-layer catalyst, or (2) using a quartz wool carrier to disperse the catalyst. The latter of these methods was used in the prototype catalytic reactor.

4.5 Test Results

A summary of all the catalyst evaluations is given in Table 5. The test conditions, the maximum conversions, and ratio of carbon to catalyst are given for most of the tests. During some of the original tests, only the conversion was determined; therefore, no values are shown for carbon/catalyst ratio.

As the catalytic disproportionation progresses, some of the surface of the catalyst is coated with carbon and becomes ineffective as a catalyst. This causes a gradual decrease in the conversion; therefore, in designing catalytic hardware, a representative average conversion must be used. Plots of this phenomenon are shown for two feed gas compositions and two flow rates in Figure 33. Fluctuations in temperature are believed to be partially responsible for some of the rapid change in conversion which is shown during a run. During the catalyst evaluation some of the runs were terminated because the pressure drop had increased to at least 3 psi rather than because conversion decreased. This was partially overcome by splitting the catalyst into several layers. The conversions of three layer catalyst tests are shown in Figure 34.

4.6 The Effect of Parameters

The operating system parameters affect the catalytic disproportionation reaction in various ways as described in the following discussion.

4.6.1 Feed Gas Composition

The concentration of carbon monoxide directly effects the conversion of CO to CO_2. Several catalysts which provided conversions approaching 90 percent with a 100 percent CO feed, gave only 30 to 40 percent conversion with a 50% CO feed. The effect of three feed gas compositions on the H-219 catalyst was noted previously in Figure 33.

Table 5 SUMMARY OF CATALYTIC DISPROPORTIONATION TESTS

Run No.	Catalyst	Flow cc/Min	Feed Gas Percent CO (Balance CO_2)	Temperature Range °F	Hours Run	Max Conversion Percent	Weight of Catalyst Grams	Weight of Carbon Grams	Ratio $\frac{\text{Carbon}}{\text{Catalyst}}$	Average Rate of Carbon Formation g/hr	Comment
1	Ni on Al_2O_3 1/8 x 1/8 pellets	100	100	100-1200		25-30	15	11	0.73		22 mm id reactor
2	Ni Powder Commercial	"	"	100-1200	3	10	40	--	--		"
3	Fe Powder Commercial	"	"	625-1080	6	80	37	--	--		"
4	1018 Steel Shavings	"	"	800-1100		55	9.9	11.3	1.14		"
5	1018 Steel Shavings H_2 Reduced	"	"	900-1000		28	10.0	10.0	1.0		"
6	1035 Steel Shavings	"	"	100-1285		30	16.6	5.0	0.3		"
7	" " "	"	"	1000-1100		45	--	6.5	--		"
8	Carbon Formed in Previous Run	"	"	600-1200		15	--	--	--		"
9	1095 Steel Shavings	"	"	75-1275	6	15	17.0	Slight	0		"
10	Cast Iron	"	"	700-1040		31	19.0	22	1.16		"
11	1018 From Run 4 Cleaned	"	"	470-1060		43	11.0	--	--		"
12	Decomposed Iron Formate	"	"	400-900		87	--	--	--		"
13	" " "	"	"	"		90	--	--	--		"
14	Decomposed Ni Formate	"	"	300-700		99	--	--	--		"
15	Decomposed Co Formate	"	"	300-800	4-1/2	98	--	--	--		"
16	Decomposed Ni Formate	"	"	300-850		98	--	--	--		"
17	" " "	"	50	"		92	--	--	--		"
18	Decomposed Fe Formate	"	100	800		87	--	--	--		41 mm id Reactor
19A	1018 Steel Strips	"	"	960		15	--	--	--		"
19B	" " "	10	"	850		70	--	--	--		"
19C	" " "	"	50	--		4	--	--	--		"
20A	Cleaned Run 19 Catalyst	100	100	740-850		65	--	--	--		"
20B	Cleaned Run 19 Catalyst	100	50			5-10	--	--	--		"
21	1095 Steel Strips	"	100			25	--	--	--		"
22A	1018 Steel Strips	"	"	900-1000		10-15	--	--	--		"
22B	Oxidized 1095 Steel Strips	"	"	950		55	--	--	--		"
23	" " "	"	"	900-1000		60-67	--	--	--		"
24 - 25	Cobalt or Nickel Strips	"	"	1000		2 - 3	--	--	--		"
26	1018 Strips Steel Rerun	"	"	910		0	--	--	--		"
27	Same Strips Cleaned	"	"	"	31	32	56.4	2	0.036	0.06	"
28	Grade 0 Steel Wool	"	"	"	53	82	2.3	15.3	6.7	0.29	"
29	" " " "	"	"	830	48	59	8.5	32.1	3.8	0.67	"
30	" " " "	"	"	930-970	51	55	8.5	25.7	3.0	0.50	"
31	Powdered Ti Carbide	"	"	930-980	20	0	19	0	0	0	"
32	Grade 0 Steel Wool	"	"	1020-1080	73	60	8.5	37	4.4	0.51	"

Table 5 Continued

Run No.	Catalyst	Flow cc/Min	Feed Gas Percent CO (Balance CO_2)	Temperature Range °F	Hours Run	Max Conversion Percent	Weight of Catalyst Grams	Weight of Carbon Grams	Ratio Carbon Catalyst	Average Rate of Carbon Formation g/hr	Comment
33	Grade0 Steel Wool	100	100	1140-1260	73	60	8.5	46	5.4	0.63	41 mm id Reactor
34	Nickel Felt	"	"	932-1035	59	10	8.0	3.2	0.4	0.05	"
35	Grade 0 Steel Wool	"	"	875-980	117	25	2.1	15.0	7.1	0.13	"
36	Grade 0 Steel Wool Oxidized	"	"	870-1030	168	55	6.3	44.2	7.0	0.26	"
37	Grade 000 Steel Wool	"	"	970-1080	32	61	5.3	25.4	4.8	0.79	"
38	" " " "	50	"	960-1140	141	69	5.5	32.0	5.8	0.23	"
39	Ni Felt Oxidized	100	"	1000	20	6.0	9.9	0.9	0.09	0.05	"
40	Grade 000 Steel Wool	10	"	950-980	104	78	6.2	13.8	2.2	0.13	"
41	Grade 000 Steel Wool Oxidized	200	"	912-1100	48-1/2	50	6	34.3	5.6	0.71	"
42	Grade 000 Steel Wool Oxidized	100	50	1100-1025	46	0	6	0.66	0.11	0.01	"
43	Fe_2O_3 Powder	100	100	820-1000	96-1/2	73	6	20.4	3.3	0.20	"
44	Steel Wool H_2O Soaked Oxidized at 1200°F	100	"	930-980	90	70	6	18.0	3.0	0.20	"
45	Hastelloy B Shavings	100	"	845-875	48	3.5	45.6	0.02	0.0	0.0004	"
46	Ni Formate on Glass Wool(Decomposed)	100	"	810-865	50	19	2.2	8.8	4.0	0.18	"
47	Ni Formate on Glass Wool	100	"	775-950	20.5	72.5	4.06	1.59	0.4	0.08	"
48	Reduced 000 Steel Wool	"	"	610-1070	45	74	10.2	7.5	0.75	0.16	"
49	Decomposed Fe Oxalate	"	"	840-1030	23-1/2	71	2.4	14.9	6.2	0.63	"
50	Decomposed Fe Formate	"	"	880-1020	18	71.5	3.25	12.4	3.8	0.69	"
51	" " "	"	"	930-990	48-1/2	85	6.3	13.8	2.2	0.28	"
52	" " "	"	"	845-1000	22-1/2	77-1/2	2.7	10.6	4.0	0.47	"
53	RUN NO GOOD - - - GAS BY-PASSING CATALYST										
54	Grade 0 Steel Wool Oxidized	100	"	995-1075	144	38.5	6.4	35.6	5.6	0.25	Reverse Flow
55	" " " "	"	"	1500-1640	143	20.5	10.4	9.8	0.94	0.07	41 mm Reactor
56	" " " "	"	"	915-980	21	78	10.3	16.8	1.6	0.80	"
57	Decomposed Ni Formate	"	"	900-1180	100	88	4.6	43.4	9.4	0.43	"
58	Oxidized/Reduced, Grade 0 Steel Wool	"	"	903-1035	74	72	9.25	29.2	3.2	0.32	"
59											
60	Raney Nickel	"	"	795-990	48	92.5	1-2 grams (Est.)	53.6	27-53 (est)	--	"
61	Raney Nickel as Slurry (dried)	"	"	730-1010	48	66	5.8	10	1.6	0.21	"
62	Raney Nickel	BLEW UP	"								
63	H-219 (Girdler)	100	"	885-985	27	96	10.0	30.3	3	1.12	"
64	Raney Nickel	"	"	950-1000	50	36	1.9	9.4	5	0.47	"
65	H-219	"	"	910-960	63-1/2	97.5	5.1	35.3	6.9	0.36	"
66	Decomposed Ni formate	"	"	730-890	48	95	15.3	46.8	3	0.97	"
67	Raney Nickel	"	"	800-950	47	95.5	7.1	34	4.8	0.72	"

Table 5 Continued

Run No.	Catalyst	Flow cc/Min	Feed Gas Percent CO (balance CO_2)	Temperature Range °F	Hours Run	Max Conversion Percent	Weight of Catalyst Grams	Weight of Carbon Grams	Ratio Carbon/Catalyst	Average Rate of Carbon Formation g/hr	Comments
68	Raney Nickel	100	100% CO	725-890	19	73	4.0	7.2	1.9	0.38	1 mm id reactor
69	Chromated Raney Nickel	"	"	800-900	73	94.5	10.6	60.0	5.7	0.82	
70	Raney Cobalt	"	"	750-880	57	95	11.4	57.6	5.1	1.0	
71	Raney Iron	"	"	735-960	24	65.5	5.2	12.8	2.5	0.53	
72	Raney Nickel	"	"	700-1020	89	98.3	10.0	60.5	6.0	0.68	
73	H-219	"	"	910-1010	19	100	10.3	14.4	1.4	0.76	
74	Raney Iron	"	"	500-915	7.5	74	19.7	9.2	.5	1.23	
75	Raney Cobalt	"	"	650-1160	47.5	96	28.4	42.6	2.1	0.60	
76	Platinum Wire Mesh	"	"	890-275	0	3.7	0	0	0	0	
77	H-219	50	"	880-910	114	94	5.0	48.6	9.7	0.42	
78	Grade 0 Steel Wool	100	"	880-1000	19	48	6.5	10.4	1.6	0.55	
79	" " " "	"	"	840-980	119	67	6.5	41.1	6.3	0.35	
80	8/14 Mesh H-219	50	"	900-980	96.1	89.5	5.0	66.2	13.3	0.69	
81	Top 5 grams of Run 80	"	"	920-960	26.5	57	4.8	8.5	1.8	0.32	
82	Raney Nickel	100	"	920-1000	58.5	85	Approx 5	32.4	6.5	0.55	
83	14/40 Mesh H-219	"	"	920-970	22.5	91	5.0	37.8	7.6	1.68	
84	Decomposed Fe Formate	"	"	890-930	22.0	70	6.0	9.1	1.5	0.41	
85	Raney Nickel	"	"	860-1020	59.5	86	2-4 (Est)	~15-17	4-8	0.25	
86	Raney Iron	"	"	760-1000	64.5	71	5.8	13.0	2.25	0.20	
87	4/8 Mesh H-219	"	"	940-1000	66.0	97	5.0	66.0	13.2	1.00	
88	4/8 Mesh H-219	50	"	970-1000	96.5	99	5.0	28.0	5.6	0.29	
89	" " "	100	50	960-1030	129.2	80	5.0	36.1	7.2	0.28	
90	" " "	"	10	830-1000	240.0	81	5.0	7.4	1.5	0.031	
91	" " "	50	50	920-1015	168	99.5	5.0	45.8	9.1	0.27	
92	4/8 Mesh H-219 (on 3 tiers)	100	100	880-1020	71.5	100	5.0	60.0	12.0	0.84	
93	" " " "	50	"	910-1030	96.5	99	5.0	55.7	11.1	0.56	
94	4/8 mesh H-219 on Stainless Wool Support	100	"	970-1030	47.5	85	5.0	55.6	11.1	1.17	
95	4/8 Mesh H-219 (on 3 tiers)	"	50	1010-1040	120	99	5.0	44.3	8.8	0.37	
96	Powder H-219 on 7.2g Steel Wool	"	100	940-1050	44.6	72	12.2	40.8	3.4	0.91	
97	Girdler G78 Pellets	"	"	930-1005	19.0	92	5.0	14.5	2.9	0.76	
98	Girdler G78 Crushed	"	"	910-1060	17.5	96	5.0	13.0	2.6	0.74	
99	H-219 on Stainless Wool	"	"	880-1050	118	100	5.0	72.2	14.5(5.2)*	0.62	
100	" " " "	50	"	930-1050	263.5	99.5	5.0	91.9	18.4(7.6)	0.35	
101	4/8 Mesh H-219 (on 3 tiers)	50	50	1020-1090	456.5	99.5	5.0	66.7	13.3	0.15	
102	H-219 on Stainless Wool	"	"	970-1050	237.5	99	5.0	43.0	8.6(4.2)	0.18	

Table 5 Continued

Run No.	Catalyst	Flow cc/min	Feed Gas Percent CO (balance CO_2)	Temperature Range °F	Hours Run	Max Conversion Percent	Weight of Catalyst Grams	Weight of Carbon Grams	Ratio $\frac{\text{Carbon}}{\text{Catalyst}}$	Average Rate of Carbon Formation g/hr	Comments
103	H-219 on Stainless Wool	100	50	970-1020	95.5	98.5	10.0	47.1	4.7 (2.4)	0.49	Sleeve Used
104	" " " "	"	"	920-1070	92.5	81.0	15.0	27.2	1.81 (1.07)	0.29	Sleeve Used Gas by-passing catalyst
105	" " " "	"	"	970-1085	96.5	44	5.0	23.6	4.7 (2.1)	0.25	
106	" " " "	"	"	970-1180	69.5	99	5.4	11.1	2.1 (0.72)	0.16	Gas By-passing
107	H-219 on Quartz Wool	"	"	970-1090	111.5	100	8.0	45.8	5.7 (3.9)	0.41	
108	" " " "	"	"	960-1065	141	100	18.5	52.7	2.9 (2.2)	0.37	

*Number in parenthesis refer to weight ratio based on weight of catalyst plus carrier.

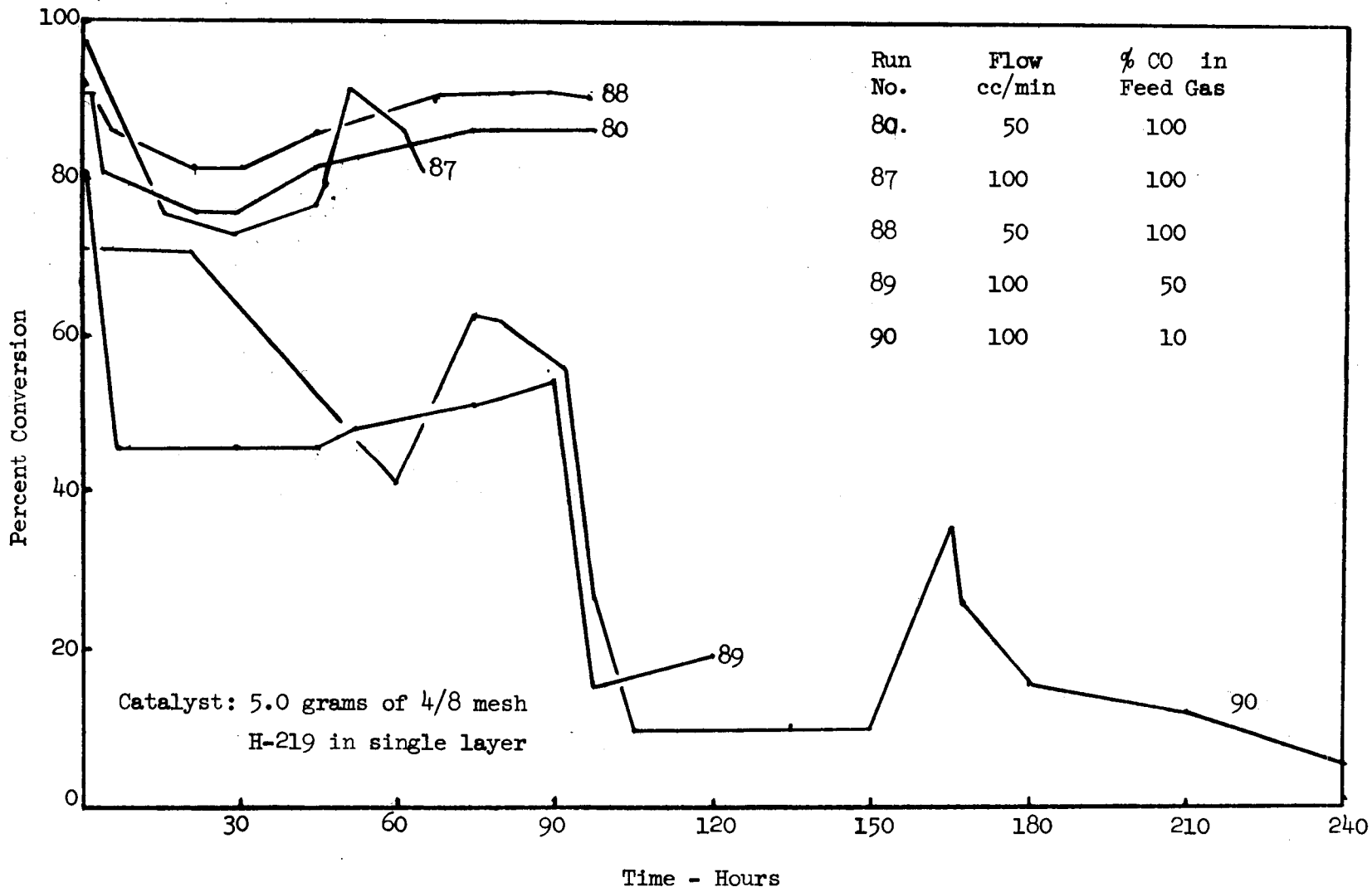

Figure 33 - CONVERSION VS. TIME FOR SINGLE LAYER OF CATALYST

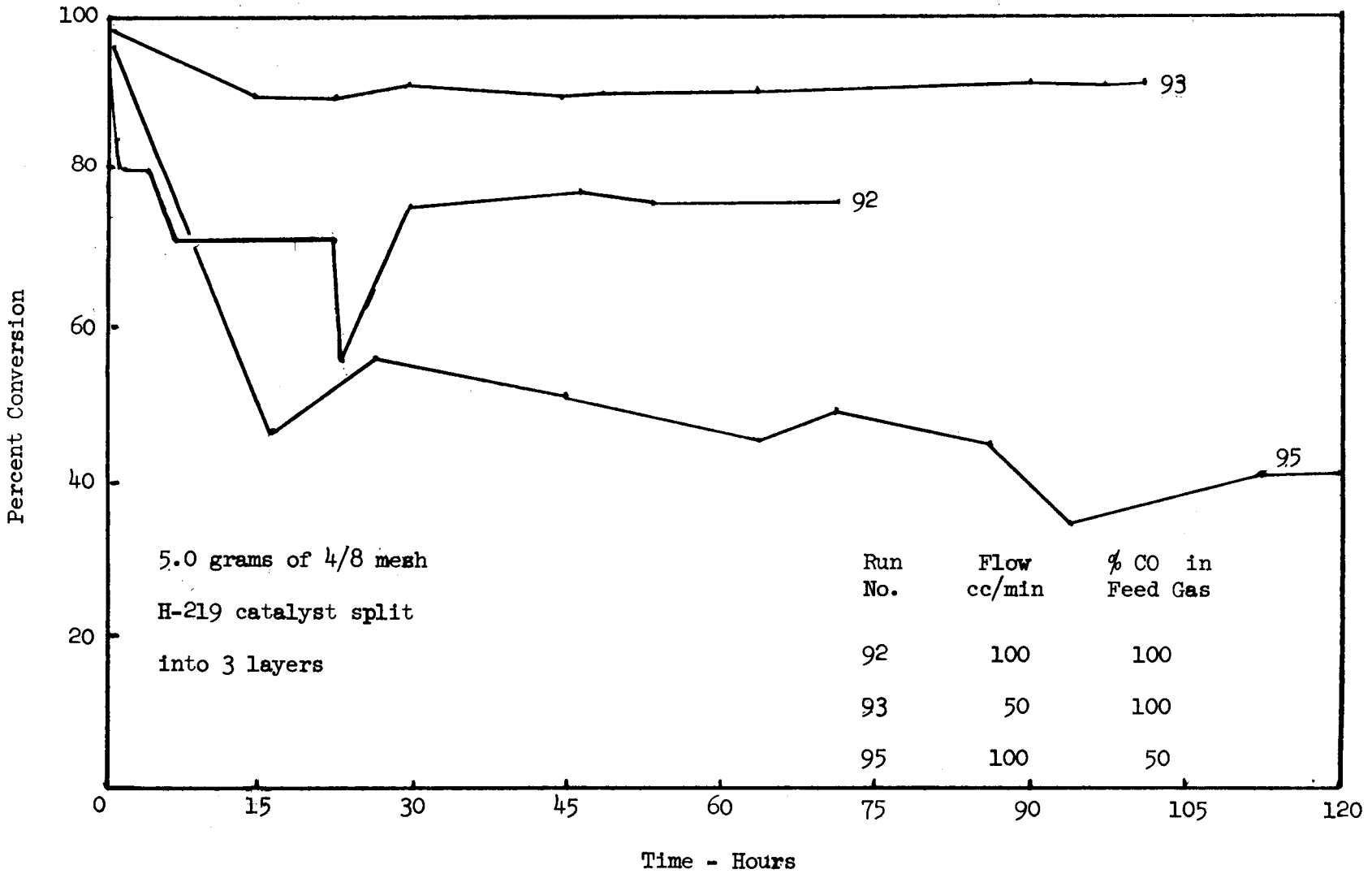

Figure 34 - CONVERSION VS. TIME FOR CATALYST SPLIT INTO 3 LAYERS

4.6.2 Temperature

The optimum temperature varies for different catalysts and the form of the catalyst. Highly active catalyst worked at temperatures as low as 600°F; however, the best overall temperature appears to be between 905° to 1050°F for the H-219 catalyst.

4.6.3 Form

The form of the catalyst significantly influences the activity of the catalyst. When the catalyst is in the form of felt, wool, or strips, iron exhibits the greatest activity and nickel is almost inactive; however, when powders or granules are used, both nickel and cobalt are more active than iron. The form also effects the conversion and the ratio of carbon to catalyst. For example, when steel is in the form of a flat strip the conversion and ratio of carbon to catalyst are lower than the conversion and ratio obtained from steel wool.

4.6.4 Flow Rate

As shown in Figures 33 and 34, the slower flow rate (50 cc/min) yields a higher percent conversion than the higher flow rate (100 cc/min). However, the higher flow rate produces a higher rate of carbon formation.

4.6.5 Pressure

Theoretically, an increase in pressure will increase the conversion because at any given temperature the reaction $2\ CO \rightarrow CO_2 + C$ has an equilibrium constant defined by:

$$K = \frac{(P_{CO_2})}{(P_{CO})^2} .$$

At higher pressures a feed gas composed of a 1:1 mixture of carbon monoxide - carbon dioxide is further from equilibrium than it is at one atmosphere and therefore has a greater driving force toward equilibrium.

4.7 Conclusion

After evaluating many types and forms of catalysts, the best one was found to be Girdler H-219 nickel oxide. This catalyst can be dispersed throughout a matrix of quartz wool to immobilize it for weightless conditions and to allow space for carbon build-up. This particular catalyst appears to be the least affected by changes in feed gas composition when compared to the other catalysts which were tested. Ratios of carbon to catalyst of 14.5:1 have been obtained with H-219 and 100 percent carbon monoxide feed gas. When the feed gas composition was decreased to 50 percent, the ratio decreased to 10:1 and when the feed contained 10 percent carbon monoxide the ratio fell to 1.5:1. Higher ratios could be obtained by simply leaving the reaction run for a longer time; however, near the end of a run the degree of conversion had usually fallen to below 20 percent or the run had ended because of excessive pressure drop caused by carbon build-up. A ratio of carbon to catalyst of approximately 30:1 was obtained during one test with Raney nickel but this run could not be duplicated.

SECTION 5

CATALYTIC REACTOR FABRICATION AND TESTING

5.1 System Design

5.1.1 Capacity

The composition of the gas entering the catalytic reactor is controlled by the performance of the electrolysis cell upstream of the reactor. Carbon dioxide is fed to the cathode side of the electrolysis cell where carbon monoxide is produced. If any carbon dioxide is left unreacted, it mixes with the carbon monoxide and passes out to the disproportionation cell. Consequently the working model of the catalytic disproportionation reactor constructed for this contract was designed for one-tenth man capacity with a feed gas composition of 50 percent carbon monoxide and 50 percent carbon dioxide.

This composition was assumed to be a realistic estimate of the gas leaving the cathode side of the carbonate electrolysis cell. Assuming that the carbon dioxide production rate of one man is 0.1 lbs per hour then the components which react or are formed in the system for one-tenth man capacity are as shown in Table 6.

Table 6

REACTANT AND PRODUCT FLOW RATES IN OVERALL SYSTEM

Component	lb/hr	cc/min (STP)
CO_2 fed to system inlet	.0100	42
O_2 formed	.0073	42
C formed	.0027	--
CO reacted to form .0027 lb carbon (absolute conversion rate in the catalytic reactor only)	.0127	83

In experiments with the H-219 catalyst, the fraction of the carbon monoxide which is reacted (percent conversion) started between 90 and 100 percent and then slowly decreased to between 40 and 80 percent as described previously (Section 4.5). At constant flow, an average conversion was used in scaling up from the glassware experiment. The average amount of carbon monoxide which reacts was not lower than forty percent of the carbon monoxide which is fed to the reactor. The CO feed rate to the reactor was thus 83/0.4 = 207 cc/min; the total flow of a 1:1 CO:CO_2 mixture would be 414 cc/min; this was rounded to 400 cc/min for testing.

At the beginning of the tests on the model reactor the capacity approximated 0.2 to 0.25 man, at the end of the run the capacity was slightly less than 0.1 man; the average capacity exceeded 0.125 man.

5.1.2 Operating Cycle

Rather than have one large reactor which would have the capacity to operate continuously for an extended period of time (such as 100 days or more), this unit was designed with a small reactor sized to operated for 7 to 8 days as described in Section 5.2. At the end of the period, the reactor would be shut down and the catalyst cartridge replaced with a fresh cartridge.

The advantages of a replaceable cartridge are (1) smaller dimensions providing less surface heat losses and (2) minimized pressure drop due to carbon build-up.

Catalytic tests in glassware were made with a reactor 12 inches long x 1.5 inches i.d. and operated for approximately 120 hours with a 1:1 carbon monoxide carbon dioxide feed at a total flow of 100 cc/minute. This same length was used in the prototype unit but the diameter was proportioned up to 3.0 inches in order to obtain the required capacity.

5.2 Reactor Assembly

A photograph of the one-tenth man capacity catalytic disproportionation reactor is shown in Figure 35. This laboratory model has controls for gas flow, heater power and temperature. The overall envelope for the unit is 19" wide x 19" deep x 35" high. The reactor is 12-1/2" long x 3.0" diameter. Figures 36 and 37 show the reactor inside of the unit with and without the heaters attached to the reactor wall. The insulation thickness is 6 inches.

5.2.1 Flow Diagram

The flow sheet in Figure 38 shows that the gas mixture of carbon monoxide and carbon dioxide is fed through a rotameter, to the catalyst bed and out of the system. In the performance tests the exit gas was passed through a Lira infrared CO analyzer and then through a Lira infrared CO_2 analyzer to determine degree of CO conversion. In an actual system the exit gas would be recycled to the gas inlet; however, for convenience during the tests, the exit gas was dumped and an analyzed gas mixture was used for the feed gas.

5.2.2 Pressure Drop

The pressure drop across the catalyst bed is measured with a Dwyer differential pressure gauge (range, 0 - 3 psi). During most of the run, the needle is not deflected because the pressure drop is less than 2" H_2O. The end of a run is signified by pressure build-up resulting from blockage of the many paths for gas flow, at this point. The pressure drop increases to several psi in a few hours.

Figure 35 CATALYTIC REACTOR

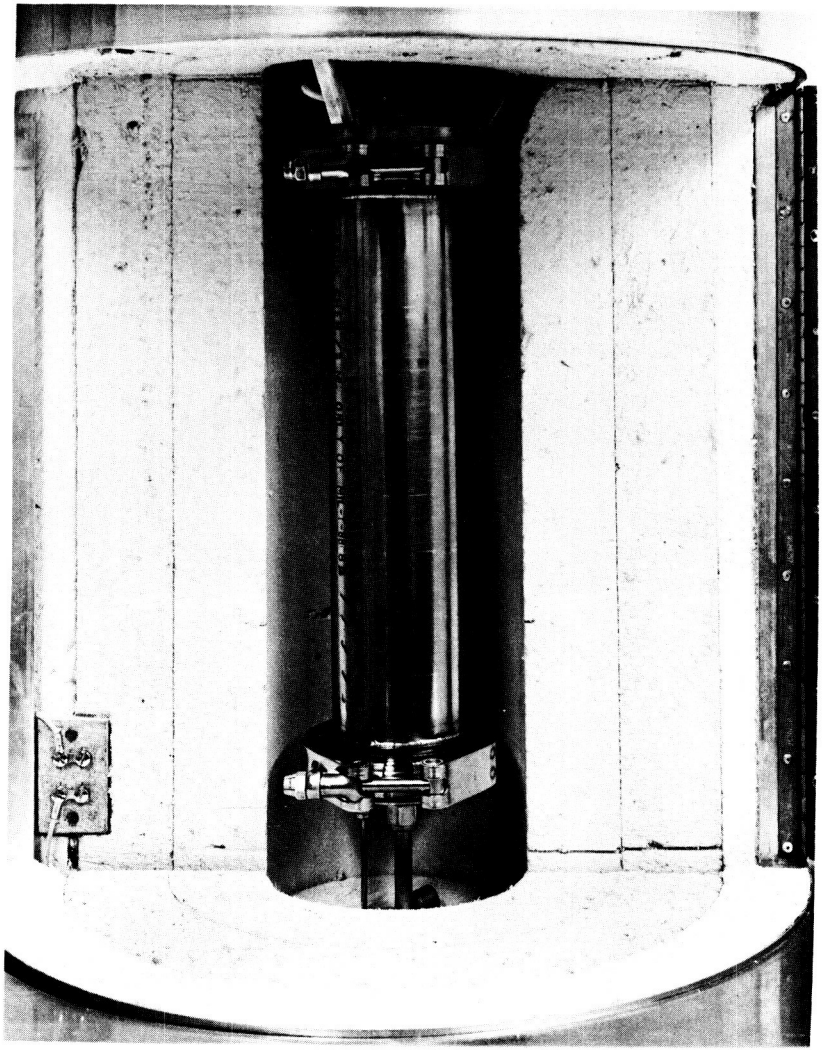

Figure 36
REACTOR INSIDE OF UNIT

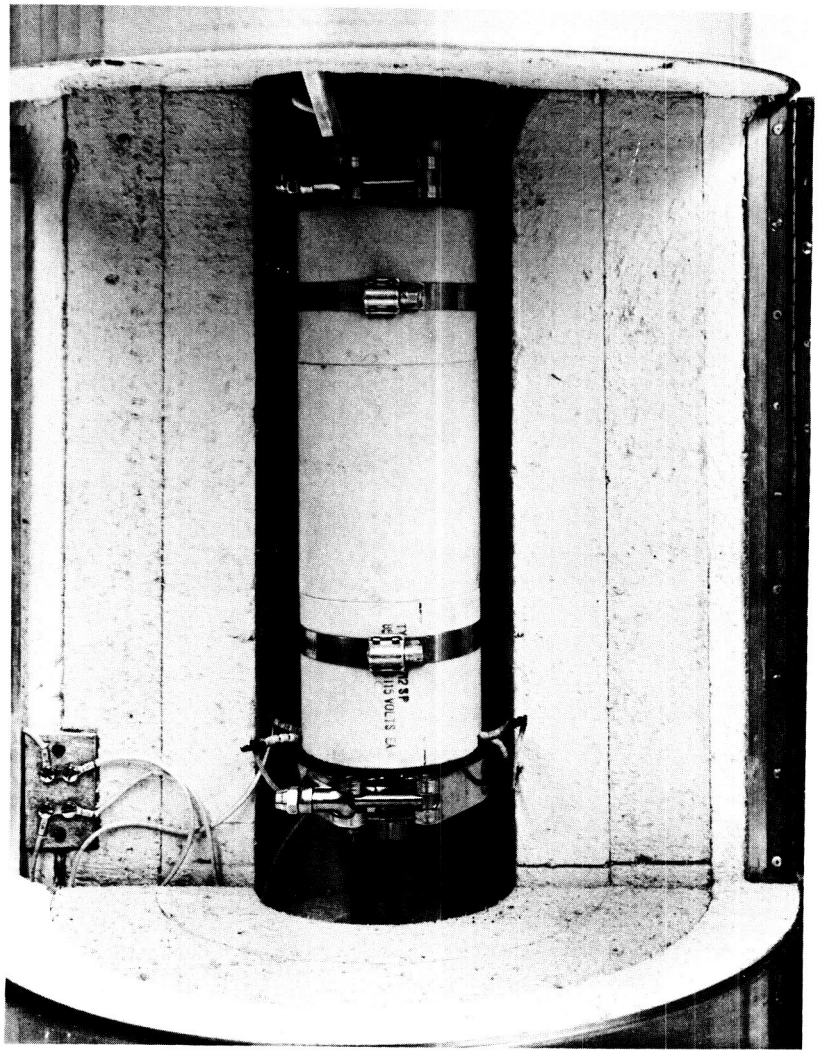

Figure 37
REACTOR WITH HEATERS ATTACHED

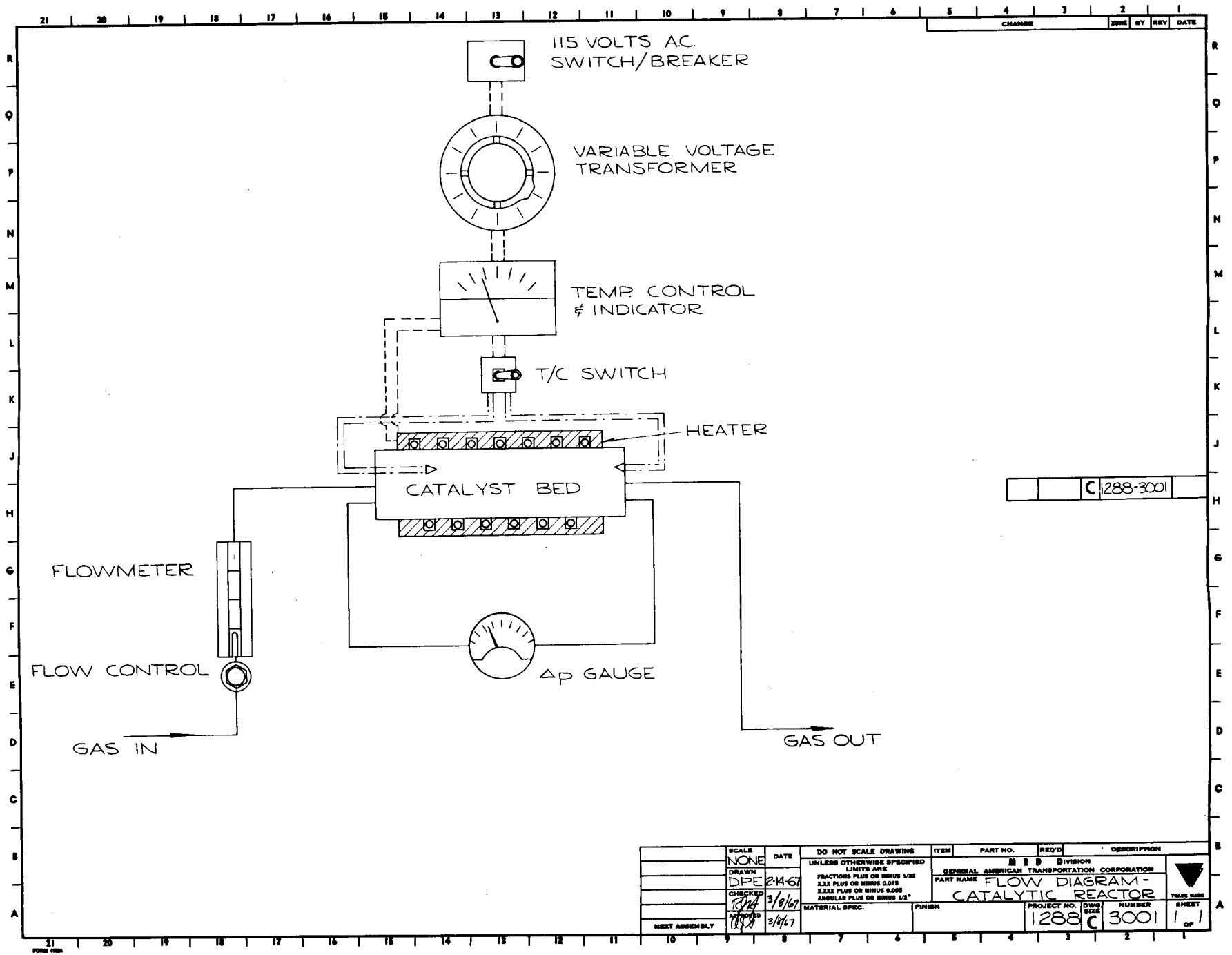

Figure 38 FLOW DIAGRAM OF CATALYTIC REACTOR

5.2.3 Reactor Canister

Two types of canisters were built for the catalytic reactor. The first, as shown in Figure 39 was constructed from a Hastelloy sheet rolled into a tube 12.5 inch long x 3.0 inch o.d. x 0.063 inch wall. Hastelloy flanges were welded to each end with seats for a filter disk and a retaining ring. The face, having concentric grooves machined in the surfaces to give more reliable seal between the end caps and the reactor, was sealed with an asbestos gasket. Hastelloy was chosen for the material of construction because it is less susceptible to carbide precipitation in the 800°/1650°F operating temperature range than is austenitic stainless steel.

The second type of reactor was made from a seamless stainless steel type 321 tube, 12.0 inch long x 3.0 inch o.d. x 0.035 inch wall; the flanges were identical to those on the first tube. This reactor was fabricated and put into operation so that performance tests could be made while awaiting delivery of the all Hastelloy reactor.

5.2.4 Heaters and Heater Control

The catalyst bed was heated with two semi-circular heating elements (Lindberg/Hevi-Duty type 3712-SP) which are clamped to the reactor canister shown previously in Figure 37. The heater power is controlled with a Powerstat variable transformer and the temperature is controlled with an API proportional controller. The sensing element is a chromel/alumel thermocouple inside of the reactor. Another thermocouple which measures the exit gas temperature is placed in the gas stream and is located at the filter element in the top (exit end) of the reactor.

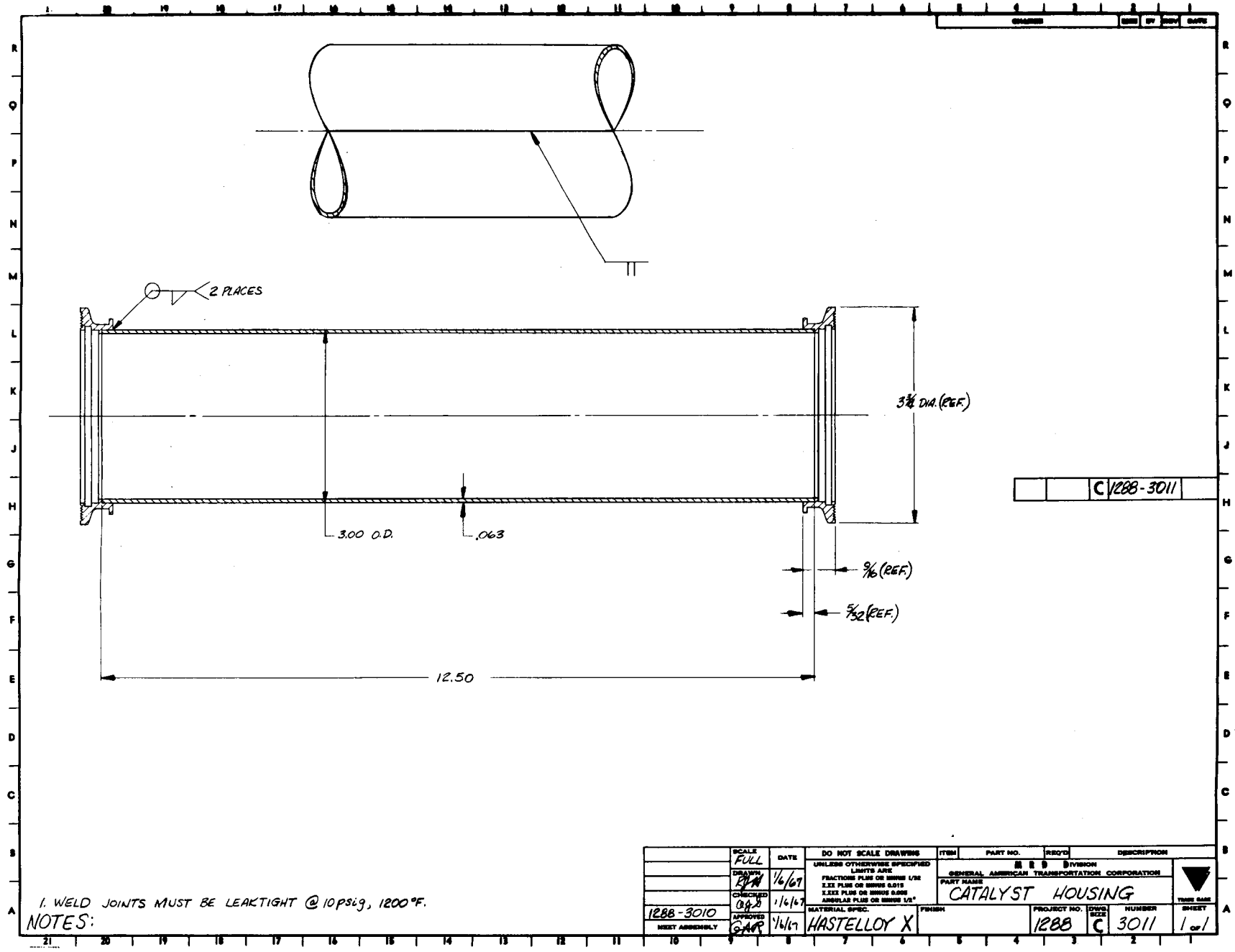

Figure 39 REACTOR CANISTER

5.2.5 Filters

A 1/8 inch thick porous aluminum oxide filter disk is mounted in the exit end of the reactor to insure that there is no carbon entrainment in the gas stream which leaves the reactor. This filter retains a 5.0 micron diameter particle. An identical filter was used on the inlet side of the reactor canister to hold the catalyst in place. A small hole was drilled in the center of this filter so that a thermocouple can be inserted in the catalyst bed.

5.2.6 Catalyst

The catalyst used in the performance tests of the laboratory model was granular Girdler H-219 nickel oxide supported on quartz wool as described in Section 4 of this report. The quantities used are described in the performance tests.

5.3 Performance Tests

The Catalytic Reactor was operated under the following conditions to verify its performance.

1.	Feed Gas Composition:	50 Percent Carbon Dioxide 50 Percent Carbon Monoxide
2.	Flow Rate:	400 cc/min (STP)
3.	Temperature:	1000 - 1020°F

5.3.1 Test 1

The reactor was loaded with 10.9 grams of quartz wool and 47.5 grams of H-219 catalyst split into three layers. The thermocouple which produces the input signal for the temperature controller was positioned in

the catalyst bed along the axis of the reactor and one inch from the bottom. This proved to be too far from the middle of the bed because the actual center of the reactor was at approximately 1300°F while this thermocouple read 1000°F. No conversion took place and the run was ended after two days; the nickel oxide catalyst was found to have been reduced to nickel and consequently no carbon had formed.

5.3.2 Test 2

The reactor was loaded with eleven grams of quartz wool and sixty grams of H-219 catalyst. This quantity of catalyst was believed to be approximately twice as much as required but was used to insure that the reaction would take place and meet the required specifications. The controlling thermocouple was inserted to the center of the reactor. The conversion (as shown in Figure 40) started at 100 percent, then dropped to approximately 60 percent until the run was ended after 194 hours (> 8 days) when the conversion was 34 percent. The initial high conversion is attributed to the chemical reaction in which carbon monoxide reduces nickel oxide to nickel. After this initial period, carbon monoxide conversion is due to catalysis alone. The average conversion for the entire run was 52.1 percent. After the reactor was disassembled, 303.5 grams of carbon were in the canister which yields an average rate of carbon formation of 1.56 grams per hour, equivalent to approximately one-eighth man capacity.

During the first 4 days of the run there was no noticeable pressure drop across the reactor (< 0.03 psi). At the end of the fifth day the Δp was 0.08 psi, at the end of the sixth it was 0.18 psi, at the end of the seventh it was

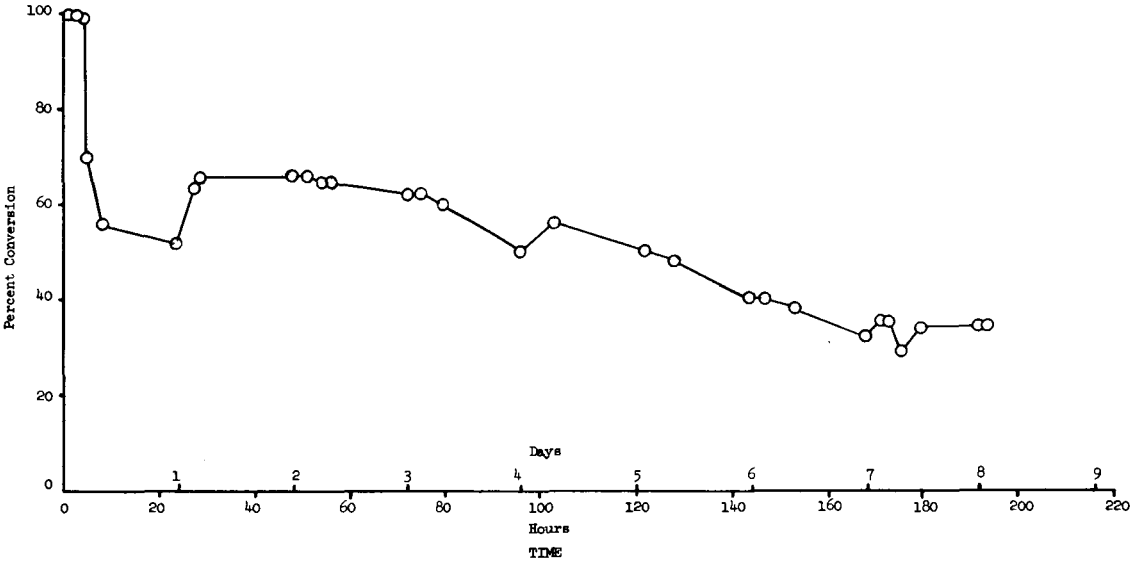

Figure 40 CO CONVERSION AS A FUNCTION OF TIME
LABORATORY MODEL CATALYTIC REACTOR
ONE-TENTH MAN CAPACITY, H-219 CATALYST

0.5 psi, and when the run was ended the Δp was 1.05 psi. The ratio of carbon to catalyst was 5.05; however, less catalyst could probably have been used with almost the same amount of carbon collected. This would increase the carbon to catalyst ratio.

5.3.3 Test 3

This test was performed to provide a time analysis for changing the reactor canister. When Test No. 2 was ended, the unit was flushed with carbon dioxide, the power was turned off, and the insulation door was opened. As soon as the exit gas analyzers indicated that all of the carbon monoxide was flushed from the system (about 5 minutes), the reactor and heater assembly

were removed; this took 45 minutes. The door was then closed to prevent unnecessary cooling of the insulation. The contents of the reactor (catalyst, quartz wool, and carbon) were removed, the reactor was repacked with fresh quartz wool and catalyst, and the reactor and heater assembly were placed in the unit. This procedure took 90 minutes. If a prepared replacement reactor had been available, the time for this procedure would have been approximately one-half hour.

Next, the power was restored, the heaters were turned on, and the reactor was again flushed with carbon dioxide. After two hours the reactor reached 1000°F, the feed gas was changed to 50 percent carbon monoxide and the reaction began. The entire shutdown time was four hours after nearly 8 days of operation, or out of a 198 hour cycle approximately 2 percent is used for switching canisters; this was equivalent to one-half hour per 24 hours of operating time, which is well within the one hour specification.

5.3.4 Carbon Entrainment

No carbon was found downstream of the reactor. The quartz wool plug at the end of the reactor and the 5.0 micron pore size ceramic filter effectively prevented carbon entrainment.

5.4 Conclusion

A laboratory type catalytic type reactor for the disproportionation of carbon monoxide into carbon and carbon dioxide was designed, built and tested. This unit provided in excess of one-tenth man capacity and surpassed all specifications.

SECTION 6

CONCLUSIONS AND RECOMMENDATIONS

The following conclusions and recommendations are based on the data obtained from the laboratory experiments with a molten carbonate electrolysis cell which converts carbon dioxide to carbon monoxide and oxygen, with a silver alloy membrane which separates oxygen from carbon dioxide, and with a prototype catalytic reactor which converts carbon monoxide to carbon dioxide and carbon.

6.1 Conclusions

6.1.1 The Electrochemical Reduction of Carbon Dioxide

The electrolysis of carbon dioxide in a molten carbonate cell produces carbon and carbon monoxide at the cathode and carbon dioxide plus oxygen at the anode at 1300°F. Ceramic coated stainless steel is not suitable for the cell housing because the carbonate attacks the ceramic glaze and the glaze becomes electrically conductive at elevated temperatures.

Silver cannot be used as an electrode because it is chemically attacked; therefore, a silver oxygen membrane cannot be placed in contact with the electrolyte. The only material which was found to perform as an anode or cathode without being corroded was platinum 10% rhodium wire gauze.

The electrolytes, which contain 34% to 50% by weight magnesium oxide, were not sufficiently fluid to prevent gas leakage across the electrolyte.

The expansion and contraction of the electrolyte when passing through the phase change from solid to liquid, causes fractures and gas leakage across the electrolyte.

6.1.2 Oxygen Permeation Through Silver

High purity silver will selectively allow oxygen permeation; however, it develops pinholes rapidly at 1300°F. A membrane with longer operating life can be fabricated from a silver alloy which contains trace amounts of nickel and magnesium. This alloy yields rates of oxygen permeation higher than the published rates for pure silver and has the capability to operate continuously for 60 days without failure.

The rate of oxygen permeation increases with increasing temperature; the temperature of the laboratory cell was limited to 1400°F by the softening point of the brazing alloy used to assemble the cell.

The rate of permeation is inversly proportional to membrane thickness. The present minimum thickness for tubes fabricated from the silver alloy with trace quantities of magnesium and nickel is approximately 0.005 inches.

6.1.3 Catalytic Disproportionation

The Girdler H-219 nickel oxide catalyst was superior to any other catalyst which was tested for the disproportionation of carbon monoxide into carbon and carbon dioxide.

The laboratory type catalytic reactor, which was fed a 1:1 mixture of carbon monoxide and carbon dioxide at a rate of 400 cc/minute, operated continuously for eight days. Four hours were required to replace the carbon filled reactor and bring the reactor back to the operating temperature of 1000°F. Because an average of 52 percent of the carbon monoxide was converted instead of an anticipated 40%, the capacity exceeded the required one-tenth man capacity.

The weight of the reactor, seals, retaining rings, and filters exceeded the weight of catalyst by a ratio of approximately 15 to 1. Therefore, an improved reactor is more important than an improved catalyst.

6.2 Recommendations

6.2.1 Electrochemical Reduction of Carbon Dioxide

Depending upon the need for another process to reduce carbon dioxide, the following problems should be solved for the molten carbonate reduction cell.

(1) A cell housing should be fabricated from impervious alumina or zirconia and the operating temperature should be increased beyond 1300°F.

(2) Sintered platinum electrodes should be substituted for the wire mesh electrodes so that a more fluid electrolyte can be used to prevent gas leakage.

6.2.2 Oxygen Permeation

The silver alloy membrane oxygen permeation cell could be scaled to a prototype unit from the laboratory data which has been obtained; however, to obtain improved performance thinner wall tubes must be fabricated and to obtain longer operating life an improved alloy must be developed. These alloys would probably be composed of silver with various small amounts of nickel, magnesium, aluminum, or palladium.

6.2.3 Catalytic Disproportionation

The catalytic reactor performed to specification but improvements can be made to improve the weight penalty of the system. The improvements

which must be developed prior to design of a flight type system are:

1. The development of a thin lightweight disposable canister. This would eliminate the need to empty a used reactor; emptying is undesireable because it is a dirty operation.

2. The optimum reactor design, operating, and ratio of carbon to catalyst must be determined to conserve weight, power, and volume.

3. The use of high efficiency, high temperature thermal insulation to significantly reduce the thickness of required insulation. Also a redesign of reactor supports to reduce the heat loss which travels to the skin of the reactor housing. This was found to be a major factor in the heat losses in the prototype model.

BIBLIOGRAPHY

Adkins, H., and Billica, H: The Preparation of Raney Nickel Catalysts and Their Use Under Conditions Comparable With Those for Platinum and Palladium Catalysts. J. Am. Chem. Soc., Vol. 70, Feb. 1948, pp 695-698.

Dushman, S.: Scientific Foundations of Vacuum Technique. Second ed., John Wiley and Sons, Inc. 1962.

Frohlich, K., Die Bedeutung des Kornwachstums beim Werkstoff Silber. Die Chemische Fabrik 12 , 1939, pp 30-33.

Gregory, E., and Smith, G.: The Effects of Internal Oxidations on the Tensile Properties of Some Silver Alloys at Room and Elevated Temperatures. Journal of the Institute of Metals 85, 1957, pp 81-87.

Mitchell, W., ed.: Fuel Cells, Academic Press, 1963.

Weissberger, A. ed.: Technique of Organic Chemistry. Vol II. Second ed. Interscience Publishers, Inc. 1956.

Winsel., A.: Beiträge zur Kenntnis der Stromverteilung in porösen Elektroden. Zeitschrift für Elektrochemie, Bd 66, Nr. 4, 1962, pp 287-304.

Young, G., ed.: Fuel Cells, Volume 2, Reinhold Publishing Corp. 1963.